

# Diffusion Models in 3D Vision: A Survey

Zhen Wang, Dongyuan Li, Renhe Jiang

**Abstract**—In recent years, 3D vision has become a crucial field within computer vision, powering a wide range of applications such as autonomous driving, robotics, augmented reality (AR), and medical imaging. This field relies on the accurate perception, understanding, and reconstruction of 3D scenes from 2D data sources like images and videos. Diffusion models, originally designed for 2D generative tasks, offer the potential for more flexible, probabilistic approaches that can better capture the variability and uncertainty present in real-world 3D data. However, traditional methods often struggle with efficiency and scalability. In this paper, we review the state-of-the-art approaches that leverage diffusion models for 3D visual tasks, including but not limited to 3D object generation, shape completion, point cloud reconstruction, and scene understanding. We provide an in-depth discussion of the underlying mathematical principles of diffusion models, outlining their forward and reverse processes, as well as the various architectural advancements that enable these models to work with 3D datasets. We also discuss the key challenges in applying diffusion models to three-dimensional (3D) vision, such as handling occlusions and varying point densities, and the computational demands of high-dimensional data. Finally, we discuss potential solutions, including improving computational efficiency, enhancing multimodal fusion, and exploring the use of large-scale pretraining for better generalization across 3D tasks. This paper serves as a foundation for future exploration and development in this rapidly evolving field.

**Index Terms**—Diffusion model, 3D vision, generative model.

## I. INTRODUCTION

In recent years, 3D vision has become a crucial field within computer vision, powering a wide range of applications such as autonomous driving, robotics, augmented reality, and medical imaging. These applications rely on accurate perception, understanding, and reconstruction of 3D scenes from 2D data sources, such as images and videos. As 3D vision tasks become more complex, traditional methods often struggle with efficiency and scalability.

Diffusion models [1]–[5], originally proposed in the field of generative modeling, have rapidly evolved and show significant potential in many areas of computer vision. These models, based on the idea of transforming data through a series of stochastic steps, have been successful in image generation [6]–[9], denoising [10], and restoration tasks [11]. In particular, diffusion models have demonstrated strong generative capabilities, allowing for the generation of high-quality, diverse outputs while maintaining robustness against noise.

In recent years, the development of diffusion models has shifted from 2D to more challenging 3D tasks [12]–[14], including 3D object generation [15]–[17], shape completion

[18], [19], and point cloud reconstruction [20], marking a new phase in both diffusion modeling and 3D vision.

Applying diffusion models to 3D vision tasks presents a promising frontier, primarily due to their ability to model complex data distributions and their inherent robustness to noise. Diffusion models provide a powerful framework for tasks that require the synthesis, completion, or enhancement of 3D data, such as shape generation [21] or depth estimation [22]. Unlike traditional 3D modeling techniques, which rely on deterministic algorithms, diffusion models offer the potential for more flexible, probabilistic methods that can better capture the variability and uncertainty present in real-world 3D data.

The growing interest in diffusion models stems from their ability to generate detailed, high-quality results in 2D tasks, leading researchers to explore their applicability in 3D. This survey aims to consolidate the state-of-the-art approaches that leverage diffusion models for 3D vision, discussing their potential benefits, such as improved accuracy in 3D reconstructions and better handling of occlusions and sparse data.

While the application of diffusion models to 3D vision holds great promise, it is not without challenges. One of the main technical hurdles is the increased complexity of 3D data, which can be represented in various forms, such as meshes, voxels, or point clouds, each with its own processing demands. Integrating diffusion models with these heterogeneous data structures remains a challenge, as does scaling the computational requirements for 3D tasks, which are often significantly more intensive than their 2D counterparts.

Another challenge lies in the difficulty of modeling long-range dependencies in 3D data, which diffusion models are not natively equipped to handle. Additionally, the scarcity of large annotated datasets for many 3D vision tasks further complicates the training of diffusion models, requiring substantial amounts of high-quality data to generalize effectively.

This survey focuses on the application of diffusion models across a wide range of 3D vision tasks, including but not limited to 3D object generation, point cloud denoising, 3D reconstruction, and scene understanding [23]. We review various diffusion model architectures and their adaptations to 3D vision, covering both early-stage and recent advancements made in the last five years. Special attention is paid to discuss how these models address the challenges specific to 3D data and the computational constraints associated with large-scale 3D vision problems. The key contributions are as follows:

- A comprehensive categorization and summary of existing work that applies diffusion models to 3D vision tasks, including their advantages and limitations.
- An in-depth analysis and comparison of various key techniques, frameworks, and methodologies used to adapt diffusion models for 3D data.

Zhen Wang is with the Institute of Innovative Research, School of Information and Communication Engineering, Tokyo Institute of Technology, Tokyo 152-8550, Japan. (zhenwangrs@gmail.com).

Dongyuan Li and Renhe Jiang are with the Center for Spatial Information Science, The University of Tokyo, Tokyo, Japan. (lidy@lr.pi.titech.ac.jp, jiangrh@csis.u-tokyo.ac.jp).

- A detailed discussion on the current challenges and open problems in the field, along with potential future research directions for improving diffusion models in 3D vision applications.
- An extensive review of relevant datasets and benchmarks used for evaluating diffusion models in 3D vision tasks.

For our survey, we employed a comprehensive literature search strategy to ensure a thorough exploration of the field. We began by identifying key terms and phrases relevant to our topic, including “diffusion models”, “3D vision”, and related concepts such as “generative models” and “neural networks for 3D data”. We conducted our search across multiple academic databases, including IEEE Xplore <sup>1</sup>, arXiv <sup>2</sup>, and Google Scholar <sup>3</sup>, focusing on publications from the last five years to capture recent advances. Additionally, we prioritized peer-reviewed journal articles, conference papers, and preprints, ensuring the inclusion of high-quality and cutting-edge research. Using this strategy, our aim was to provide a comprehensive and up-to-date survey of diffusion models in 3D vision.

The rest of the paper is organized as follows. Section II provides an overview of diffusion models, including their theoretical foundations and key developments in 2D and 3D vision tasks. Section III dives into the core concepts of 3D vision, discussing various data representations and their challenges. Section IV presents a detailed review of diffusion models applied to different 3D vision tasks. In Section V, we summarize the available datasets and benchmarks used for evaluation. Finally, Section VI discusses future directions and open problems, followed by a conclusion in Section VII.

## II. DIFFUSION MODEL FUNDAMENTALS

### A. Introduction to Diffusion Models

1) **Definition of Diffusion Models:** Diffusion models [1], [3] are a class of generative models that learn to generate data by gradually transforming random noise into structured data. This process involves a forward diffusion process, where noise is added step by step to the data, and a reverse process that denoises and reconstructs data from pure noise. Their purpose is to model the data distribution through iterative denoising, and they have been shown to produce high-quality samples across various domains, including 3D vision.

2) **Historical Context and Evolution:** Diffusion models were first introduced as stochastic processes inspired by non-equilibrium thermodynamics [24]. Early works [25] laid the foundation for probabilistic diffusion modeling. Over time, these models evolved, particularly with the introduction of *Denoising Diffusion Probabilistic Models (DDPMs)* by Ho et al. [1], which improved scalability and sampling efficiency.

3) **Key Characteristics:** Diffusion models are unique due to their iterative process, which involves two main components:

- **Forward Process:** Gradual addition of Gaussian noise to the data.
- **Reverse Process:** A learned denoising process that reverses the noise to generate new samples.

This framework allows diffusion models to avoid mode collapse, a common issue in other generative models like GANs, and produce high-quality, diverse samples.

### B. Mathematical Foundations of Diffusion Models

1) **Forward Diffusion Process:** The forward diffusion process is a Markov chain where Gaussian noise is incrementally added to the data at each time step. Given an initial data point  $\mathbf{x}_0$ , the noisy version at time  $t$  is denoted as  $\mathbf{x}_t$ , and the process can be formulated as:

$$q(\mathbf{x}_t|\mathbf{x}_0) = \mathcal{N}(\mathbf{x}_t; \sqrt{\alpha_t}\mathbf{x}_0, (1 - \alpha_t)\mathbf{I}),$$

where  $\alpha_t$  is a noise schedule that controls the amount of noise added at each time step.

2) **Reverse Process:** The reverse process involves learning a denoising function  $p_\theta(\mathbf{x}_{t-1}|\mathbf{x}_t)$  that estimates the posterior distribution of the previous step,  $\mathbf{x}_{t-1}$ , given the current step  $\mathbf{x}_t$ . The reverse process can be written as:

$$p_\theta(\mathbf{x}_{t-1}|\mathbf{x}_t) = \mathcal{N}(\mathbf{x}_{t-1}; \mu_\theta(\mathbf{x}_t, t), \Sigma_\theta(\mathbf{x}_t, t)).$$

This learned model progressively denoises the sample until it reaches a final clean data point  $\mathbf{x}_0$ .

3) **Probability Densities and Score Matching:** Diffusion models approximate the data distribution by modeling the gradients of the data’s log-probability, also known as the *score function*  $\nabla_{\mathbf{x}} \log p(\mathbf{x})$ . The reverse process is closely linked to score matching, which optimizes the model by matching the score of the data distribution with that of the learned model. The score matching loss is typically written as:

$$\mathcal{L}_{\text{score}} = \mathbb{E}_{q(\mathbf{x}_t|\mathbf{x}_0)} \left[ \|\nabla_{\mathbf{x}_t} \log q(\mathbf{x}_t|\mathbf{x}_0) - \nabla_{\mathbf{x}_t} \log p_\theta(\mathbf{x}_t)\|^2 \right].$$

This method also connects to variational inference through the minimization of a KL divergence term between the true data distribution and the modeled distribution.

4) **Loss Functions:** The primary objective in diffusion models is to learn the reverse process by minimizing the *denoising score matching loss*. One common form of the loss is:

$$\mathcal{L}_{\text{denoise}} = \mathbb{E}_{t, \mathbf{x}_0, \epsilon} \left[ \|\epsilon - \epsilon_\theta(\mathbf{x}_t, t)\|^2 \right],$$

where  $\epsilon_\theta(\mathbf{x}_t, t)$  is the model’s prediction of the added noise  $\epsilon$ , and  $t$  is uniformly sampled from the diffusion time steps.

### C. Variants of Diffusion Models

1) **Denoising Diffusion Probabilistic Models:** Denoising Diffusion Probabilistic Models (DDPM) [1] are one of the most well-known variants of diffusion models. In DDPMs, the forward process gradually adds Gaussian noise to the data, transforming the original data distribution into a known prior (usually a standard Gaussian distribution). The reverse process, parameterized by a neural network, is trained to denoise the corrupted data step-by-step. The forward process can be described as:

$$q(\mathbf{x}_t|\mathbf{x}_{t-1}) = \mathcal{N}(\mathbf{x}_t; \sqrt{1 - \beta_t}\mathbf{x}_{t-1}, \beta_t\mathbf{I}), \quad (1)$$

<sup>1</sup><https://ieeexplore.ieee.org/Xplore/home.jsp>

<sup>2</sup><https://arxiv.org/>

<sup>3</sup><https://scholar.google.com/>

where  $\mathbf{x}_t$  is the data at step  $t$ , and  $\beta_t$  is a variance schedule controlling the noise level at each timestep.

The reverse process is learned via:

$$p_\theta(\mathbf{x}_{t-1}|\mathbf{x}_t) = \mathcal{N}(\mathbf{x}_{t-1}; \mu_\theta(\mathbf{x}_t, t), \Sigma_\theta(t)), \quad (2)$$

where  $\mu_\theta(\mathbf{x}_t, t)$  and  $\Sigma_\theta(t)$  are the predicted mean and variance, parameterized by a neural network. By optimizing a variational lower bound, DDPMs achieve high-fidelity image generation.

2) **Score-Based Generative Models:** Score-based generative models [3] differ from DDPMs by estimating the gradient of the log-likelihood of the data distribution, known as the score function  $\nabla_{\mathbf{x}} \log p(\mathbf{x})$ . The score-based framework is applied in both denoising score matching and generative models. The forward process involves adding noise to the data, similar to DDPMs, but the key difference is the reverse process, which is driven by the score function:

$$\nabla_{\mathbf{x}} \log p_t(\mathbf{x}) \approx s_\theta(\mathbf{x}, t), \quad (3)$$

where  $s_\theta(\mathbf{x}, t)$  is the score network trained to approximate the true score at different noise levels.

The reverse process can be described as solving a differential equation parameterized by the score network:

$$d\mathbf{x} = -\frac{1}{2}s_\theta(\mathbf{x}, t)dt + \sqrt{dt}\mathbf{z}, \quad \mathbf{z} \sim \mathcal{N}(0, \mathbf{I}). \quad (4)$$

Score-based models have been applied to generate 3D data, such as point clouds and meshes, by learning the underlying structure of 3D objects and ensuring high-quality reconstructions in 3D vision tasks.

3) **Stochastic Differential Equations:** Stochastic Differential Equations (SDEs) [26] offer a continuous-time formulation of diffusion models. Instead of discrete timesteps, as in DDPMs, SDEs evolve data continuously over time. The forward process can be described as an Itô SDE:

$$d\mathbf{x} = f(\mathbf{x}, t)dt + g(t)d\mathbf{w}, \quad (5)$$

where  $f(\mathbf{x}, t)$  is the drift function,  $g(t)$  is the diffusion coefficient, and  $d\mathbf{w}$  is the Wiener process.

The reverse SDE for generation follows:

$$d\mathbf{x} = [f(\mathbf{x}, t) - g(t)^2 \nabla_{\mathbf{x}} \log p_t(\mathbf{x})]dt + g(t)d\mathbf{w}, \quad (6)$$

where  $\nabla_{\mathbf{x}} \log p_t(\mathbf{x})$  is the score function. This continuous-time formulation allows for more flexible control over the diffusion process, and it has been successfully applied in 3D generative tasks, such as generating point clouds and voxel grids.

4) **Other Variants:** Other variants of diffusion models include hybrid approaches that combine elements of both discrete and continuous models, as well as models that integrate different noise distributions beyond Gaussian. For example, some models utilize mixture noise distributions or extend diffusion models for different types of data, such as text or multimodal inputs.

Another extension involves conditioned diffusion models [27], where the generative process is conditioned on additional

information, such as class labels or semantic guidance, allowing for controlled synthesis of 3D data. Conditional diffusion models have been especially useful in tasks like conditional 3D object generation and scene completion.

#### D. Generative Process in 3D Vision

1) **Diffusion Models vs. Other Generative Models:** Compared to GANs [28] and VAEs [29], diffusion models offer advantages like better sample diversity, avoidance of mode collapse, and smoother interpolations. While GANs are often faster in generating samples, diffusion models are known for their superior ability to generate high-quality, detailed 3D structures.

2) **Advantages of Diffusion Models in 3D Vision:** In 3D vision, diffusion models excel due to their ability to generate smooth, continuous surfaces and handle complex, high-dimensional data. They are particularly advantageous in applications requiring detailed geometry, such as 3D shape reconstruction, where mode collapse in GANs and blurry outputs in VAEs are often problematic.

### III. 3D VISION FUNDAMENTALS

#### A. 3D Representation

Three-dimensional data representation forms the cornerstone of 3D vision, providing the means to model, analyze, and interact with complex spatial information. In an era where applications such as augmented reality (AR), virtual reality (VR), and advanced robotics are increasingly prevalent, a robust understanding of 3D representation is essential for interpreting and manipulating the physical world. The representation of 3D data can take various forms, each with distinct characteristics, advantages, and limitations.

1) **2D Representations:** 2D representations leverage two-dimensional images to infer and reconstruct three-dimensional information. These representations are particularly useful for rendering and understanding 3D scenes but rely heavily on the quality and number of 2D inputs for accuracy.

a) **Depth Map:** A depth map [30] represents the distance from a particular viewpoint (often a camera) to objects in the scene as a 2D image, where each pixel's value corresponds to the depth (or distance) to the nearest surface. Depth maps are commonly generated from stereo vision, structured light, or time-of-flight (ToF) cameras, which estimate depth based on the geometry of light or motion. Depth maps offer an efficient way to encode 3D information in a format that is easy to integrate with traditional 2D image processing techniques. They are particularly useful in applications like 3D reconstruction, scene understanding, and robotic navigation, where understanding the spatial layout of a scene is essential. In addition, depth maps can be used in conjunction with RGB images to create RGB-D datasets, which combine both color and depth information for more comprehensive scene analysis. One limitation of depth maps is that they typically represent only the visible surfaces of objects from a single viewpoint. This means that occluded areas (i.e., parts of objects that are hidden from the camera) are not captured, which can pose challenges for certain 3D reconstruction tasks.

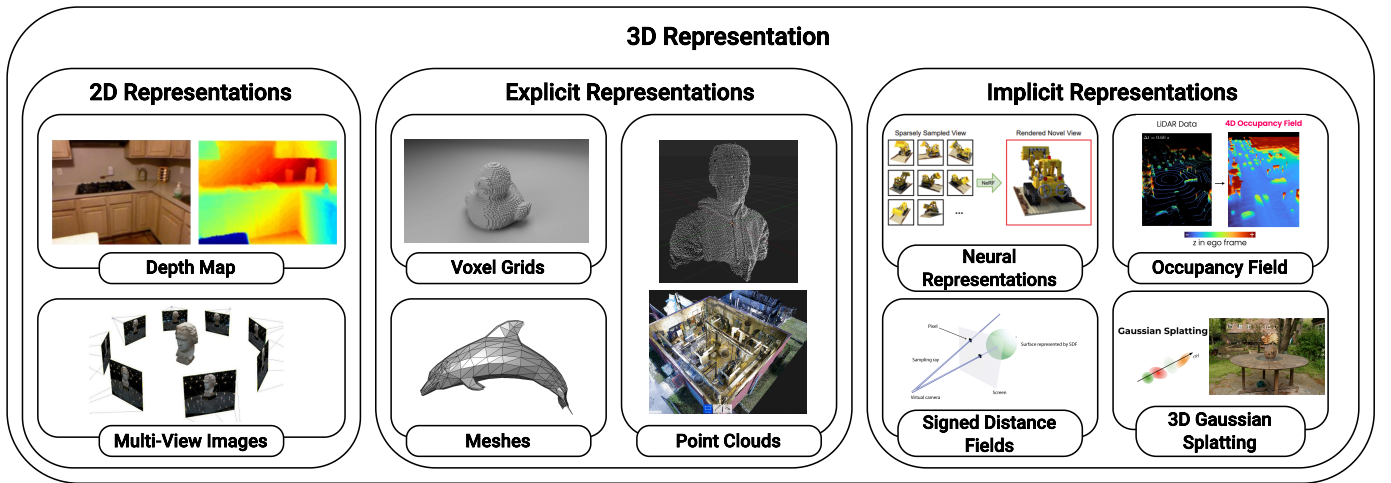


Fig. 1. 3D representations.

*b) Multi-View Images:* Multi-view images [14], [31] refer to multiple 2D images of the same scene or object taken from different perspectives. These images can be used to infer 3D information using techniques like stereo matching or structure-from-motion (SfM). The idea is to leverage the differences in appearance across views (known as parallax) to recover the geometry of the scene. Multi-view images are widely used in 3D reconstruction, virtual reality (VR), and augmented reality (AR) applications, where they help create immersive, real-world-like experiences. In photogrammetry, for instance, multiple overlapping images of a scene are analyzed to generate detailed 3D models. Similarly, in autonomous driving, multi-view images from multiple cameras mounted on a vehicle are used to perceive the surrounding environment in 3D. Compared to other 3D representations, multi-view images maintain high fidelity in appearance, as they capture real-world textures directly from images. However, they require sophisticated algorithms for accurate depth estimation and 3D reconstruction, and managing a large number of images can lead to high computational complexity.

*2) Explicit Representations:* Explicit representations directly define the geometric shape of 3D models, providing clear and detailed structures. These representations are intuitive and easy to manipulate, but they often require significant storage space, especially for complex shapes.

*a) Point Clouds:* Point clouds [32] represent 3D objects or scenes by sampling points in three-dimensional space. Each point in a point cloud is characterized by its spatial coordinates ( $x, y, z$ ) and can optionally include additional attributes such as color, normal vectors, or intensity values. Point clouds are a direct output of many 3D scanning devices like LiDAR, structured light scanners, or stereo vision systems. Point clouds offer a sparse representation of a surface, capturing only the sampled points rather than continuous surfaces. While simple and efficient for storing raw geometric data, point clouds often lack the topological information needed to define object surfaces or relationships between points, making it harder to perform tasks like rendering or simulation without further processing. To enhance their usability, point clouds are often

converted into more structured forms such as meshes or voxel grids. Point cloud data is widely used in various applications, including autonomous driving (for environment perception), robotics (for navigation and mapping), and 3D reconstruction (for scanning objects or scenes).

*b) Voxel Grids:* Voxel grids [33] discretize 3D space into small, equally sized cubic units known as "voxels" (volume elements), which are analogous to pixels in 2D images. Each voxel represents a small portion of space and can hold properties like occupancy (whether the voxel contains part of an object), color, or density. Voxel grids are particularly advantageous for applications requiring volumetric analysis or when it's necessary to explicitly model the interior and exterior of objects, such as medical imaging (e.g., CT or MRI scans), volumetric rendering, and certain physics simulations. One key advantage of voxel grids is their regular structure, which makes them amenable to direct use in 3D convolutional neural networks (3D CNNs) for tasks such as object classification, segmentation, and scene understanding. However, voxel grids can be computationally expensive due to the cubic growth of data size with resolution, which can lead to high memory requirements for detailed objects or large scenes. To mitigate this, techniques like octrees, which hierarchically represent voxels at different resolutions, are often used to reduce the computational burden while preserving geometric details.

*c) Meshes:* Meshes [34], [35] represent 3D surfaces using interconnected vertices, edges, and faces, typically forming polygons (most often triangles or quadrilaterals). Meshes are widely used in computer graphics, 3D modeling, and gaming due to their efficiency in representing complex surfaces with a relatively low number of data points. Each vertex in a mesh corresponds to a point in 3D space ( $x, y, z$ ), and the edges define the connections between vertices, forming the structure of the object. The faces, typically composed of triangles or quads, form the surfaces that define the shape of the object. Meshes are especially efficient for rendering, as they allow for smooth and detailed surface representation while minimizing the amount of data needed compared to volumetric representations. Meshes are not only used for visu-

alization but also for simulations involving physical properties like deformations, collisions, and animations. Moreover, they are an integral part of 3D printing workflows, where the mesh defines the boundary of the object to be printed. Mesh simplification techniques can also be applied to reduce the complexity of a mesh while retaining important geometric features, making meshes versatile for both high-precision and real-time applications.

3) **Implicit Representations:** Implicit representations define 3D structures through mathematical functions rather than direct geometry. These representations are compact and can efficiently capture complex shapes, but decoding them into explicit geometry can be more challenging.

a) **Neural Implicit Representations:** Neural implicit representations [36] are a powerful approach to encoding 3D geometry using neural networks. They represent shapes not through explicit vertices and faces, but as continuous functions that can be queried at any point in 3D space. This method allows for high levels of detail and smooth surface representations, making it particularly suitable for complex shapes. One of the key advantages of neural implicit representations is their ability to learn from various input data, such as 2D images, point clouds, or voxel grids, enabling them to capture intricate details and variations in geometry effectively.

b) **Occupancy Field:** An occupancy field [37] is a specific type of neural implicit representation that determines whether a point in 3D space is occupied by a surface or not. This is typically modeled as a binary function where each point returns a value indicating occupancy (1) or non-occupancy (0). By training on 3D data, such as point clouds or volumetric data, occupancy fields can learn to approximate complex surfaces and provide a compact representation of the object. This representation is particularly useful in applications like scene understanding and object reconstruction, as it allows for efficient querying and rendering of surfaces.

c) **Signed Distance Fields:** Signed Distance Fields (SDFs) [38] are a popular form of implicit representation that encode the geometry of 3D shapes based on the distance from a given point to the nearest surface. The SDF function returns negative values for points inside the object, zero at the surface, and positive values for points outside. This characteristic allows SDFs to provide smooth and continuous representations of surfaces, making them ideal for tasks like shape blending, deformation, and collision detection. SDFs are also beneficial in applications such as 3D shape generation and rendering, as they can be efficiently used in ray marching algorithms to visualize complex shapes.

d) **3D Gaussian Splatting:** 3D Gaussian splatting [39] is an emerging technique that utilizes Gaussian functions to represent 3D geometry in a probabilistic manner. In this approach, each point in space is associated with a Gaussian blob, which can be combined with other Gaussian representations to form a more complex shape. This method enables the modeling of intricate details and soft boundaries, providing a more organic representation of surfaces. 3D Gaussian splatting is particularly advantageous in scenarios where data is sparse or noisy, as it inherently incorporates uncertainty and smoothness. Applications of this technique include volumetric

rendering, scene reconstruction, and enhancing neural rendering methods.

## B. Deep Learning Methods in 3D Vision

Deep learning has transformed 3D vision by enabling powerful tools for analyzing and interpreting 3D data across diverse applications such as autonomous driving, robotics, and augmented reality. This section reviews key deep learning methods for 3D vision, discussing their strengths and challenges.

1) **Convolutional-based Neural Networks:** 3D CNNs [40] extend traditional 2D CNNs to volumetric data, making them suitable for processing voxel grids. They are highly effective in capturing spatial relationships in 3D, and have been used in applications such as medical imaging and object recognition. However, the high memory and computational requirements of 3D CNNs can limit their scalability. Multi-view CNNs address this limitation by processing multiple 2D views of a 3D object and aggregating the extracted features. This technique, employed in models like MVCNN, is particularly useful for object recognition tasks in 3D spaces. Another variation, spherical CNNs, operates on spherical projections of 3D data, which is useful for rotation-invariant object recognition.

2) **Direct Point Cloud Processing Methods:** Direct point cloud processing networks analyze raw point cloud data without converting it to intermediate formats like voxels or meshes. PointNet [41] pioneered this approach by treating point clouds as unordered sets and learning features using shared multi-layer perceptrons (MLPs). PointNet++ [42] extends this by incorporating local neighborhood structures to better capture fine-grained geometric details. VoxelNet [33] combines point cloud data with voxelization, enabling both grid-based processing and direct point learning. KPConv, a more recent method, improves upon PointNet++ by using deformable convolutions on point clouds, which allows for better handling of non-uniformly distributed points.

3) **Graph Neural Networks:** Graph Neural Networks (GNNs) [43] are particularly well-suited for 3D data represented as graphs, such as meshes or point clouds with spatial relationships. MeshCNN, for example, processes triangular mesh representations, directly leveraging graph structures to perform tasks such as mesh classification and segmentation. EdgeConv, a GNN-based architecture, dynamically constructs graphs from point clouds to capture local geometric structures and inter-point relationships, making it effective for 3D object classification and segmentation. Dynamic Graph CNN (DGCNN) extends this idea by updating the graph dynamically as learning progresses, improving robustness to noisy data and object deformations.

4) **Occupancy Networks and DeepSDF:** Occupancy Networks [44] and Signed Distance Functions (SDF)-based models [45] offer implicit representations of 3D shapes. Occupancy Networks learn to predict whether any given point in space is inside or outside the shape, enabling continuous and flexible 3D surface representation. DeepSDF [45], on the other hand, models the signed distance to the closest surface for each point, offering more precise reconstructions. Another emerging

technique is Neural Radiance Fields (NeRF) [36], which represents a scene as a continuous volumetric field using implicit representations. NeRF has shown exceptional results in novel view synthesis and is gaining traction in 3D shape representation tasks.

5) **Transformer-based Architectures:** Transformers [46], originally developed for sequential data in natural language processing, have been adapted for 3D vision due to their ability to capture long-range dependencies and relationships between unordered sets. The Point Transformer [47] applies self-attention mechanisms directly to point cloud data, allowing it to learn both local and global context effectively. Similarly, 3D-DETR [48] leverages transformer-based architectures for 3D object detection. By using queries to interact with spatial features, transformers have demonstrated strong performance on tasks like object detection and 3D scene understanding.

### C. Challenges in 3D Vision

1) **Occlusion:** Occlusion is a major challenge in 3D vision as it arises when parts of an object are obscured by other objects in the scene. This issue is particularly problematic in densely cluttered environments, where multiple objects overlap or block each other. In such cases, 3D sensors like LiDAR or stereo cameras may not capture all surfaces of the occluded object, resulting in incomplete or distorted data. The missing information makes it difficult for downstream tasks such as object recognition, surface reconstruction, or scene understanding. Various techniques, such as multi-view aggregation, depth completion, and occlusion-aware models, have been developed to mitigate this issue, but occlusion remains a challenging problem, particularly in real-time applications like autonomous driving or robotic navigation, where dynamic objects can continuously block parts of the scene.

2) **Varying Point Density:** In 3D vision, the point clouds generated by scanning devices often suffer from varying point density. Some regions of a scanned object or scene may have dense sampling, while other regions may be sparsely populated with points. This variability is influenced by factors such as the distance from the sensor to the object, the angle of incidence of the scanning beam, and the reflective properties of surfaces. For example, objects close to the sensor or directly facing it may have dense point coverage, while those further away or at oblique angles may have fewer points. This non-uniformity can lead to challenges in 3D surface reconstruction, feature extraction, and object detection. Algorithms for point cloud up-sampling, surface interpolation, and non-uniform sampling compensation are used to address this issue, but the trade-off between computational complexity and real-time performance remains a concern, especially in large-scale environments.

3) **Noise and Outliers:** Noise and outliers are inherent challenges in 3D data acquisition, often caused by limitations in sensor precision or environmental factors. Noise refers to small deviations in the position of points due to inaccuracies in the scanning process, while outliers are points that are erroneously placed far from their true locations, possibly resulting from reflections, sensor calibration errors, or environmental interference. These imperfections can distort the shape

and structure of 3D objects, leading to unreliable data for further processing. Techniques such as denoising filters, outlier removal algorithms, and robust statistical methods have been developed to handle these issues. However, finding the right balance between eliminating noise and preserving important details in the 3D data remains challenging, especially in applications like medical imaging or high-precision industrial inspections, where accuracy is critical.

## IV. 3D DIFFUSION GENERATION TASKS

This section provides an overview of various tasks involved in 3D diffusion generation, which leverage advanced machine learning techniques to create, manipulate, and analyze 3D data. These tasks are driven by the capability of diffusion models to learn complex data distributions, making them effective for generating and refining 3D content.

### A. Unconditional Generation

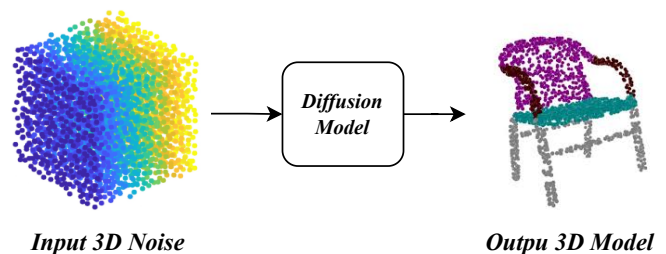


Fig. 2. Example of unconditional 3D generation task.

Unconditional 3D generation refers to the process of generating three-dimensional shapes or objects without being guided by any specific input or condition, such as a class label, image, or textual prompt. In this approach, the model learns to create diverse 3D structures based on patterns it has identified from training data, often starting from random noise or latent variables. This technique is used to synthesize new 3D shapes, scenes, or models in applications like 3D design, virtual environments, and gaming. The goal is to produce realistic and varied 3D outputs by capturing the underlying data distribution without external guidance.

Zhou et al. [15] introduce a new framework called Point-Voxel Diffusion, which is one of the earliest works to utilize diffusion models for generating 3D objects. This method combines denoising diffusion models with a probabilistic generative model of 3D shapes represented as point-voxel mixtures. It generates 3D shapes by performing a series of denoising steps that reverse diffuse the observed point cloud data back to Gaussian noise.

Ren et al. [16] observe that in the early stages of the diffusion process, the attention mechanism has a greater impact on the generation of the overall shape, while in the later stages, convolution operations significantly influence the local surface quality of the generated point cloud. Therefore, they propose a time-varying denoising model that combines convolution and Transformer architectures. This model rebalances global and local features by generating optimizable masks at each time step, enabling dynamic feature fusion throughout the process.

Zheng et al. [49] introduce a novel diffusion model-based pre-training method for point clouds called PointDif, aimed at enhancing the performance of point cloud models in downstream tasks such as classification, segmentation, and detection. PointDif treats the point cloud pretraining task as a conditional point-to-point generation problem and proposes a recurrent uniform sampling optimization strategy, enabling the model to recover uniformly from different noise levels.

Shim et al. [13] propose a two-stage 3D shape generation framework called SDF-Diffusion. In the first stage, a low-resolution SDF of the 3D shape is generated. Then, this low-resolution SDF is used as a condition for the second stage, where a diffusion model is employed for super-resolution processing to produce a high-resolution SDF. Since this method uses SDF as the representation of the 3D shape, it allows for direct mesh reconstruction using the Marching Cubes algorithm and CNNs.

Mo et al. [17] introduce a new method called DiT-3D, which converts point clouds into voxel representations and utilizes DDPMs to perform denoising operations on the voxelized point clouds, thereby generating high-quality 3D shapes. The authors initialize DiT-3D using a pretrained DiT-2D model from ImageNet and fine-tune it to enhance performance in 3D generation tasks.

Müller et al. [50] introduce a method called DiffRF, which operates directly on the radiance field representation of 3D objects, using a 3D DDPM model to generate radiance fields directly on an explicit voxel grid. This method leverages 3D supervision and volumetric rendering to guide the generation process, enabling the unconditional synthesis of high-fidelity 3D assets.

Shue et al. [51] introduce a novel 3D-aware generative model called Triplane Diffusion, designed for generating neural fields. The researchers convert 3D training scenes into a set of 2D feature planes (referred to as triplanes) and then train directly on these representations using existing 2D diffusion models to generate high-quality and diverse 3D neural fields. This approach leverages the powerful capabilities of 2D diffusion models and applies them to 3D shape generation, achieving state-of-the-art 3D generation results across multiple ShapeNet object categories.

Koo et al. [52] introduce a cascaded diffusion model called SALAD (Shape PART-Level LATent Diffusion Model), based on part-level implicit 3D representations, where each part is described by an independent embedding vector, which includes both external parameters (such as position and size) and internal attributes (such as geometric details). SALAD first learns diffusion in the lower-dimensional subspace (external parameters) and then performs conditional diffusion in the higher-dimensional subspace (internal attributes), enabling high-quality 3D shape generation with flexible editing capabilities.

Chou et al. [18] propose Diffusion-SDF, a method for 3D shape generation and completion. It uses SDFs as the 3D representation, where various signals (e.g., point clouds, 2D images) are parameterized by a neural network to capture their geometry. By modulating SDFs as 1D latent vectors and using these latent vectors as training data, the model learns

the reverse diffusion process by predicting denoised vectors to generate samples from Gaussian noise.

Nam et al. [53] propose a method called 3D-LDM for generating neural implicit representations of 3D shapes. The authors first construct a latent space of 3D shapes based on Signed Distance Functions (SDFs) by training an auto-decoder. This auto-decoder associates each shape with a latent vector, enabling the encoding and decoding of shapes. Subsequently, 3D-LDM applies a diffusion model in the latent space of the 3D shape auto-decoder, allowing for the generation of 3D shapes with continuous surfaces.

Vahdat et al. [54] introduce a novel 3D shape generation model called LION. LION uses a Variational Autoencoder (VAE) framework that incorporates a hierarchical latent space, which includes a vector-valued latent representation for the global shape and a latent space for the point cloud structure. The core of LION involves training two levels of denoising diffusion models (DDMs) within these latent spaces to generate 3D shapes.

Zhang et al. [21] introduce a new 3D shape representation method called 3DShape2VecSet, which combines concepts from Radial Basis Functions (RBF), cross-attention, and self-attention. This representation is suitable for transformer processing and can be used for neural fields and generative diffusion models. The authors also propose a two-stage model: the first stage involves an autoencoder that encodes 3D shapes into a latent space, while the second stage trains a diffusion model within the learned latent space. This approach achieves outstanding performance across various 3D shape generation and reconstruction tasks.

Lyu et al. [19] introduce a new conditional point diffusion refinement paradigm called Point Diffusion-Refinement (PDR), which is among the first to apply diffusion models to point cloud completion task. PDR first uses a DDPM to generate a coarse completed point cloud, and then applies a Refinement Network to further refine the results.

Kasten et al. [55] introduces a method called SDS-Complete, which utilizes a pre-trained text-to-image diffusion model along with the textual semantics of a given incomplete point cloud of an object to achieve a complete surface representation of the object. SDS-Complete can complete various objects at test time through optimization without the need for expensive 3D data collection, allowing the algorithm to generalize to objects that perform poorly in the training set or in real-world settings.

Nunes et al. [20] propose a LiDAR scene completion method based on DDPMs that operates directly on point cloud data rather than relying on voxel grid representations. The authors redefine the denoising scheme used in DDPMs by locally adding noise to each point instead of normalizing the input data to a noise range. This approach enables the model to learn detailed structural information of the scene effectively.

## B. Image to 3D

Image-to-3D generation focuses on converting 2D images into 3D representations. Diffusion models can help infer depth, structure, and texture from one or more 2D views, producing

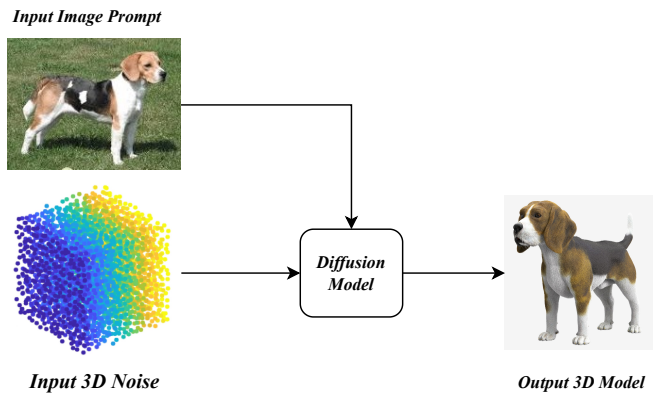


Fig. 3. Example of image to 3D generation task.

accurate 3D reconstructions. This task is pivotal in applications like 3D reconstruction from images or enhancing single-view 3D predictions by progressively refining the model’s understanding of spatial structure. Recent works have explored using diffusion models to tackle the challenging task of reconstructing 3D objects from single images. Diffusion models provide powerful generative priors that can help constrain this ill-posed inverse problem.

Wang et al. [56] propose a method called Score Jacobian Chaining (SJC), which applies the chain rule to multiply the gradients of the diffusion model with the Jacobian matrix of a differentiable renderer, thus aggregating 2D image gradients into 3D asset gradients. This enables the use of pretrained 2D diffusion models for 3D generation tasks without requiring additional 3D data.

Xu et al. [57] propose a CLIP-guided sampling strategy that effectively combines the prior knowledge of the diffusion model with a reference image. This method enables the reconstruction of realistic, 3D-consistent objects from a single image without requiring precise depth estimation. Additionally, they introduced scale-invariant depth supervision, reducing the need for accurate multi-view consistent depth estimation.

Szymanowicz et al. [58] propose a method called Viewset Diffusion, which uses multi-view 2D data to train a diffusion model for generating 3D objects. By integrating a bijective mapping between the viewset and the 3D model within the denoising network itself, the method ensures that the generated viewset and the 3D model are geometrically consistent.

Melas-Kyriazi et al. [59] propose RealFusion, in which they utilize the prior captured in the diffusion model to make up for the missing information. By optimizing a specific text prompt, they enabled the diffusion model to generate other possible views of a given object, reconstructing a 360° 3D model of the object from a single image. This achieved high-quality 3D reconstruction of arbitrary objects without 3D supervision.

Liu et al. [60] utilize 2D diffusion models to generate multi-view images, combined with a cost volume-based neural surface reconstruction method to reconstruct 3D meshes from multi-view predictions. This approach enables the rapid reconstruction of high-quality 3D mesh models from a single image, significantly reducing reconstruction time while more

accurately capturing the details and structure of the input image.

Liu et al. [61] first fine-tunes a 2D diffusion model to predict a consistent set of images from six viewpoints, providing coherent views for 3D reconstruction. It then employs a 3D diffusion model under multi-view conditions to predict a textured mesh from the consistent multi-view images, using a coarse-to-fine approach. By leveraging multi-view images as supervision and applying lightweight optimization techniques, the method enhances the texture quality of the generated mesh.

Hu et al. [62] introduce EfficientDreamer, a novel method for 3D content creation that first employs a new 2D diffusion model to generate a composite image containing four orthogonal view sub-images based on a given text prompt, which provides a strong geometric structure prior and enhancing 3D consistency. Subsequently, a 3D synthesis fusion network integrates the orthogonal view diffusion model with a pre-trained 2D diffusion model to address the “Janus problem” (the problem of multi-facetedness) in text-driven 3D generation, significantly improving the stability of the generation process and the quality of the 3D content.

Long et al. [63] introduce a cross-domain diffusion model for generating multi-view normal maps and corresponding color images, aimed at enhancing the geometric details and visual consistency of the generated results. It also incorporates a multi-view cross-domain attention mechanism and a geometry-aware normal fusion algorithm to facilitate information exchange between different views and modalities, thereby improving the consistency and quality of the generated outputs.

Tang et al. [64] propose a method called Make-It-3D, which leverages 2D diffusion models as 3D priors. Through a two-stage optimization pipeline, it first optimizes NeRF by combining constraints from the reference image and the diffusion prior on new views. Then, it transforms the rough model into a textured point cloud and further enhances realism using the diffusion prior, while also utilizing high-quality textures from the reference image to create high-fidelity 3D objects.

Zheng et al. [65] present a two step diffusion model-based 3D shape generation framework called LAS-Diffusion, in which the occupancy-diffusion first generates a low-resolution occupancy field to approximate the shape’s shell and then a SDF-diffusion synthesizes a high-resolution signed distance field within the occupancy voxels to extract fine geometric details. Notably, the authors employ a novel view-aware local attention mechanism that utilizes 2D image patch features to guide the learning of 3D voxel features, significantly enhancing local controllability and the model’s generalization ability.

Lin et al. [66] present Consistent123, which consists of two stages. In the first stage, it leverages 3D structural priors for extensive geometric utilization and incorporates a CLIP-based case-aware adaptive detection mechanism. The second stage introduces 2D texture priors, which gradually take a dominant guiding role to refine the details of the 3D model. Throughout the optimization process, the model emphasizes 3D structure guidance while progressively highlighting the importance of 2D priors over time to optimize texture details, achieving

higher quality 3D reconstruction.

Qian et al. [67] introduce a method called Magic123 for generating high-quality 3D mesh models from a single unposed image. Magic123 employs a two-stage optimization process, first optimizing a neural radiance field (NeRF) to produce a rough geometric shape, and then using a memory-efficient differentiable mesh representation to generate a high-resolution mesh. In both stages, the generation of new views is guided by combining 2D and 3D diffusion priors, with a trade-off parameter that controls the exploration (more imaginative) and exploitation (more precise) of the generated geometry.

Tang et al. [68] distinct from previous methods reliant on NeRF and transformers, employs 3D Gaussian splatting and introduce a new 3D representation method called multi-view Gaussian features, which can be fused together for differentiable rendering. And it presents a novel framework that utilizes multi-view Gaussian features and an asymmetric U-Net backbone to quickly generate high-resolution 3D models from single-view images or text prompts.

Xu et al. [69] introduce a novel feedforward 3D generation model called GRM (Gaussian Reconstruction Model) designed for efficiently reconstructing and generating 3D assets from sparse view images. At its core, GRM employs a Transformer-based network architecture that converts input pixels into 3D Gaussian values aligned with the pixels. These Gaussian values are then reprojected to form a set of densely distributed 3D Gaussian values that represent the geometry and appearance of the scene. This method not only enhances the quality and efficiency of reconstruction but also demonstrates potential in generation tasks, such as text-to-3D and image-to-3D.

Diffusion models show great promise as generative priors to address the ambiguity in reconstructing 3D objects from limited 2D supervision. Key ideas include incorporating differentiable rendering into the denoising process and using large 2D diffusion models to synthesize novel views.

Xu et al. [70] introduce InstantMesh, which aims to rapidly generate high-quality 3D mesh models from a single image while ensuring that the generated models possess good scalability for training and diverse geometric appearances. The authors combine an off-the-shelf multi-view diffusion model with a sparse-view reconstruction model based on the Large Reconstruction Model (LRM) architecture to generate consistent multi-view images, and then directly predict the 3D mesh using the LRM framework.

Liu et al. [71] propose a model called MeshDiffusion. To address the issue of irregular topology across different object categories, they utilize Deformable Tetrahedral Grids to represent 3D meshes. The model is based on Score-Based Generative Modeling, and it is trained directly on the parametric representation of 3D meshes. By training a diffusion model, MeshDiffusion generates 3D meshes effectively.

### C. Text to 3D

Text-to-3D generation involves generating 3D models or scenes directly from textual descriptions. Diffusion models are particularly suited for this task due to their ability to bridge the gap between language and 3D structure, enabling the creation

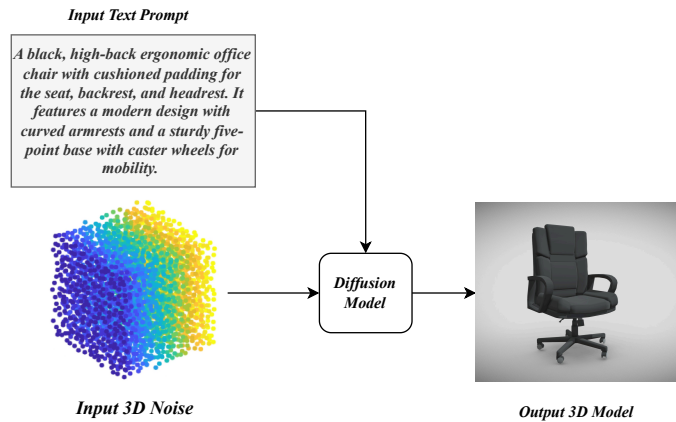


Fig. 4. Example of text to 3d generation task.

of semantically meaningful 3D assets. This is highly relevant for content creation in areas such as gaming, virtual reality, and product design.

Nichol et al. [72] is one of the first to explore how to use DDPMs to efficiently generate 3D point clouds from natural language descriptions. The authors first use a text-to-image diffusion model to generate a single synthetic view, followed by a second conditional diffusion model to produce the 3D point cloud based on the generated image.

Li et al. [73] introduce a novel 3D modeling framework called Diffusion-SDF, aimed at addressing the challenging task of text-to-shape synthesis. The authors propose a patch-based SDF autoencoder that maps the truncated signed distance fields (TSDFs) of 3D shapes into local Gaussian latent representations. And they introduce a voxelized diffusion model to capture local information and the relationships between patches (patch-to-patch) and the global structure (patch-to-global).

Metzer et al. [74] present a novel NeRF model called Latent-NeRF, which operates in latent space instead of the standard RGB space. This approach eliminates the burden of encoding the rendered RGB images into latent space at each guidance step. The authors utilize text features as another input in the latent space for text-based guidance, enhancing the model's ability to generate 3D representations based on textual descriptions.

Chen et al. [75] introduce a method called Fantasia3D, which achieves high-quality conversion from text prompts to 3D content creation by decoupling the modeling of geometry and appearance. Text features are specifically employed in the modeling of both geometry and appearance, guiding the generation process to produce the desired outcomes effectively.

Wu et al. [76] introduce a model named STPD, which generates 3D shapes and colors through a staged diffusion process. Initially, features from text and sketches are extracted separately. Multi-head attention is then employed to fuse the features from the sketch and text. Following this, a staged diffusion model is used to first generate the shape, and subsequently, colors are assigned based on the shape generated in the first stage.

Poole et al. [77] explore how to utilize a pretrained 2D text-to-image diffusion model to synthesize 3D models without requiring 3D training data. They employ a pretrained 2D text-to-image diffusion model as a prior and propose a loss function based on probabilistic density distillation. This approach allows the use of the 2D diffusion model as an prior. Finally, they optimize a randomly initialized 3D NeRF through gradient descent, aiming to achieve low loss from 2D images rendered from random viewpoints. This approach effectively addresses the challenges of scarce 3D data and the inefficiencies of 3D denoising architectures, presenting a novel possibility for 3D content creation.

Lu et al. [78] propose a novel multi-view 2.5D diffusion model, which fine-tunes a pretrained 2D model to directly capture the structural distribution of 3D data while retaining the strong generalization capabilities of the original 2D diffusion model. This approach addresses the limitations of current methods, which either rely on pretrained 2D diffusion models with time-consuming SDS or directly use 3D diffusion models constrained by limited 3D data, sacrificing diversity in generation.

Seo et al. [79] investigate the issue that 2D diffusion models lack an understanding of 3D space, often resulting in distorted and incoherent 3D scenes. To tackle this, the authors propose a new framework called 3DFuse. The framework first generates a rough 3D point cloud based on text prompts and projects it into arbitrary views to create rough depth maps. These depth maps serve as explicit 3D consistency conditions, which are fed into the 2D diffusion model. This enables the model to optimize each viewpoint in a 3D-aware manner, improving the coherence and structure of the generated 3D scenes.

Wang et al. [80] propose a novel method called Variational Score Distillation (VSD). VSD is a particle-based variational framework that models 3D parameters as random variables, contrasting with the constants used in traditional Score Distillation Sampling (SDS). By optimizing the distribution of the 3D scene, VSD aims to make the image distribution rendered from all views closely match the distribution defined by the pretrained 2D diffusion model. This approach enhances the flexibility and accuracy of 3D content generation by leveraging the strengths of both variational inference and diffusion models.

Bahmani et al. [81] introduce a technique called Hybrid Score Distillation Sampling (SDS). This method employs an alternating optimization process, beginning with the generation of an initial static 3D scene using a 3D-aware text-to-image model that avoids the ‘‘Janus problem’’. Following this, the process alternates between variational SDS and text-to-image model supervision to enhance the scene’s appearance. Finally, the technique incorporates video SDS and text-to-video model supervision to introduce motion into the scene, resulting in a dynamic and visually compelling 3D representation.

Huang et al. [82] identify a conflict between the 3D optimization process and the uniform timestep sampling in diffusion models, which led to slow convergence, poor quality of generated 3D models, and low diversity in generation. To address these issues, the paper proposes a Time Prioritized Score Distillation Sampling (TP-SDS) strategy. This approach

uses a monotonically decreasing function to prioritize different diffusion timesteps during the 3D optimization process, aligns the 3D optimization process more effectively with the sampling steps.

Chen et al. [83] introduce GSGEN, a novel method for text-to-3D generation using 3D Gaussian scattering. The method employs a two-stage optimization strategy. In the first stage, it utilizes joint guidance from 2D and 3D diffusion priors to shape a 3D-consistent coarse structure. In the second stage, during appearance refinement, the model enhances details through a compactness-based densification process

Ling et al. [84] propose a new method for generating high-quality 4D dynamic scenes from textual descriptions by leveraging dynamic 3DGS and composite diffusion models. The authors use dynamic 3D Gaussian Mixtures and deformation fields as the backbone for 4D representation. The deformation fields capture scene dynamics and transform the set of 3D Gaussians to represent object motion. The approach combines text-to-image, text-to-video, and 3D-aware multi-view diffusion models, providing feedback within a score distillation-based synthesis framework.

Yi et al. [85] explore how to efficiently generate 3D Gaussian representations from text prompts while maintaining 3D consistency and detailed generation. The authors propose a framework called GaussianDreamer, which bridges 3D and 2D diffusion models through Gaussian splatting. In this framework, the 3D diffusion model provides an initialization prior, and the 2D diffusion model enhances both the geometry and appearance, resulting in a detailed and coherent 3D output.

#### D. Texture Generation

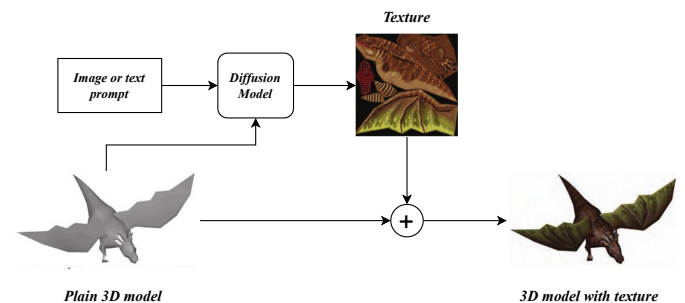


Fig. 5. Example of texture generation task.

Mesh generation involves creating polygonal meshes that define the structure of 3D objects, while texture generation refers to mapping realistic surface details onto those meshes. Diffusion models aid in both processes by generating high-fidelity meshes and textures from learned distributions. These models can ensure geometric accuracy and surface detail that align with real-world appearances, benefiting applications in graphics, simulation, and AR/VR environments.

Cao et al. [86] introduce TexFusion, which achieves text-guided 3D texture synthesis by using a latent diffusion model and a novel 3D-consistent diffusion model sampling scheme. This method runs a 2D denoising network across different 2D rendered views and aggregates the predicted results into a

latent texture map after each denoising iteration. This approach effectively generates textures with rich details and consistency, responding to text prompts, offering new possibilities for AI-based texture generation for 3D assets.

Chen et al. [87] employ a pretrained depth-aware image diffusion model, which can generate high-resolution partial textures based on text prompts. Additionally, the authors progressively synthesize high-resolution local textures from different viewpoints to avoid the accumulation of inconsistencies and stretched artifacts between views.

Yu et al. [88] investigate methods for automatically generating high-fidelity and geometry-compatible texture images on 3D mesh models. The authors propose Point-UV Diffusion, a two-stage coarse-to-fine framework that combines denoising diffusion models with UV mapping. First, a point diffusion model is used to synthesize low-frequency texture components, introducing a style-guided mechanism to address color distribution bias in the dataset. These colored points are then mapped to 2D UV space, and 3D coordinate interpolation is used to generate a rough texture image, which maintains 3D consistency and continuity.

Gupta et al. [89] propose an architecture called 3DGen, which combines a VAE and a conditional diffusion model to generate high-quality textured and non-textured 3D meshes. It consists of two stages: first, a Triplane VAE encodes the point cloud from the input mesh into a triplane Gaussian latent space, learning to reconstruct continuous textured meshes from this latent space. Next, a diffusion model is trained to generate triplane features.

Richardson et al. [90] use a pretrained depth-to-image diffusion model to render 3D models from different viewpoints, incorporating a dynamic trimap segmentation technique. By considering trimap segmentation, it proposes an improved diffusion process for generating seamless textures across various views. This enables text-guided texture generation, transfer, and editing for 3D models, significantly enhancing the quality and speed of texture generation.

Chen et al. [91] introduce SceneTex, which aims to address the problem of texture synthesis for indoor scenes. Unlike previous methods, SceneTex formulates the texture synthesis task as an optimization problem in RGB space. By employing a multi-resolution texture field and a cross-attention decoder, it effectively leverages the depth-to-image diffusion prior to generate high-quality, style-consistent textures for indoor scenes.

Li et al. [92] aim solve the infinite possibilities of UV mapping problem when generating 2D texture maps in traditional 2D diffusion methods, while using point clouds helps to avoid variations caused by different mesh topologies and UV mappings. They proposes an octree-based diffusion model (TexOct), which uses an octree structure to efficiently represent the point cloud sampled from the surface of a given 3D model. This method directly optimizes texture generation in 3D space, effectively addressing texture errors caused by self-occlusion and texture degradation due to sparse sampling.

Yeh et al. [93] research how to transfer highly detailed and complex textures from real-world environments onto arbitrary objects. They introduce TextureDreamer, a novel framework

by combining personalized modeling, score distillation, and geometry guidance, enabling it to extract texture information from a small number of images and transfer it onto target objects with different geometries.

Zeng et al. [94] introduce Paint3D, which aims to address the challenge of generating high-quality textures without embedded lighting information. By utilizing a pretrained 2D image diffusion model and a specially designed UV completion and upscaling diffusion model, Paint3D achieves the goal of generating high-quality, lighting-free 3D texture maps from text or image inputs.

Wang et al. [95] propose a novel convolution and DDPM-based reconstruction model, CRM, which leverages geometric priors and an efficient network architecture to achieve fast generation of high-fidelity 3D textured meshes from a single image.

Zhang et al. [96] propose a novel approach to achieve multi-view consistency. This method is based on a pre-trained diffusion model, such as DDIM, which decodes the predicted noise-free latent states into color space at each denoising step and blends them to form a texture image. An optimization process is then used to update the latent codes, ensuring that the images rendered from the blended texture image remain consistent across all views.

Zhang et al. [97] propose a new diffusion model that takes into account the given lighting environment during training to generate shading results under specific lighting conditions. By applying the same ambient lighting during the material extraction process, DreamMat can produce high-quality PBR materials that are consistent with the given geometry and free from any baked shadow effects.

## E. Human Avatar Generation

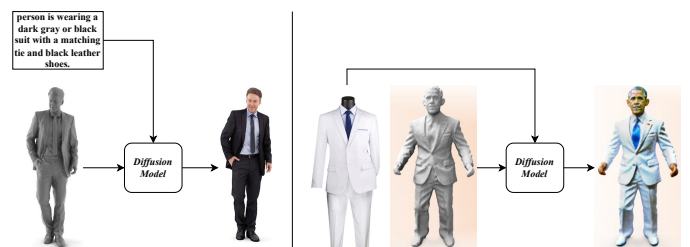


Fig. 6. Example of 3D human avatar generation task.

Human avatar generation involves creating realistic or stylized 3D models of humans. Diffusion models help generate human avatars with accurate anatomical proportions, dynamic poses, and textures. These models can also be fine-tuned for facial expressions or body movements, making them valuable for applications in gaming, virtual reality, and digital fashion.

Wang et al. [98] investigate how to use diffusion models to generate high-fidelity 3D digital avatars, represented in NeRFs. Their RODIN model effectively generates detailed 3D digital avatars by unfolding 3D feature maps onto a 2D plane and applying 3D-aware convolutions which accounts for the projection relationship of 3D data onto the 2D plane.

Jiang et al. [99] propose a method called AvatarCraft, which uses diffusion models as guidance to generate 3D human

avatars with parameterized shape and pose control based on text prompts. By mapping the target character mesh to a template character mesh through an explicit deformation field, the neural implicit field is deformed, simplifying the animation and deformation of the generated avatars. This method also supports high-quality novel view synthesis, scene composition, and animation.

Chen et al. [100] present a novel 3D deformation diffusion model capable of generating 3D mesh models based on input parameters such as identity and expression. By combining the 3D deformation model with a multi-view consistency diffusion approach, the model achieves the generation of controllable and realistic 3D avatars from a single image.

Lei et al. [101] propose the DiffusionGAN3D framework, which combines a pretrained 3D generative model (such as EG3D) with a text-to-image diffusion model. The framework employs Relative Distance Loss to enhance diversity during the domain adaptation process and utilizes case-specific learnable triplanes to improve the network’s generative capabilities.

Li et al. [92] address several key issues present in existing facial texture generation methods, including low texture quality, loss of identity information, and inadequate handling of occlusions. To tackle these challenges, the authors propose UV-IDM, which leverages the powerful texture generation capabilities of latent diffusion models (LDM) to generate realistic facial textures based on the Basel Face Model (BFM). To preserve identity information during the reconstruction process, an Identity Condition Module (ICM) is designed, allowing any outdoor image to serve as a robust condition for the LDM to guide texture generation.

Zhou et al. [102] introduce a new method called UltrAvatar, which uses Diffuse Color Extraction Model and Authenticity Guided Texture Diffusion Model to generate realistic and animatable 3D avatars from text prompts or a single image.

Chen et al. [103] introduce the first diffusion model-based framework for 3D human generation called PrimDiffusion. The authors propose a 3D human representation method based on volumetric primitives, modeling the human body as multiple small volumes with radiance and motion information. By directly manipulating the denoising and diffusion processes on the volumetric primitives, the framework addresses the high computational cost of 3D representations and the complexity of 3D human topology.

Kim et al. [104] present a 3D human generation pipeline called Chupa, aimed at addressing the challenge of generating realistic 3D human meshes with diverse identities, poses, and random details. The researchers break the problem down into 2D normal map generation and normal map-based 3D reconstruction, improving computational efficiency and generating multi-view consistent 3D models. First, a pose-conditioned diffusion model is used to simultaneously generate realistic front and back normal maps of the character. Then, mesh optimization is employed to “sculpt” an initial SMPL-X mesh to match the details of the normal maps

Svitov et al. [105] propose a method called DINAR, which creates realistic and controllable 3D cartoon characters from a single image while maintaining rendering quality and good generalization to new poses and viewpoints. DINAR combines

neural textures with the SMPL-X human model, achieving realistic quality while keeping the cartoon characters easy to manipulate and enabling fast inference. A latent diffusion model is used to recover the textures.

Kolotouros et al. [106] propose a method for generating realistic and animatable 3D human avatars solely from text descriptions. A statistical human model is then incorporated to enhance the realism of the human body structure, appearance, and deformations. Additionally, the quality of the generated models is improved by adding details to perceptually important body areas, such as the face and hands.

Ho et al. [107] introduces a new 3D human reconstruction pipeline called SiTH, which addresses the challenge of reconstructing realistic and detail-rich 3D human models from a single-view image. The SiTH method breaks down the single-view reconstruction problem into two subproblems: generating the illusion of a back view image and mesh reconstruction. First, an image-conditioned diffusion model is used to predict the appearance of the back view of the input image. Then, using both the foreground and back view images as guidance, the method reconstructs a textured mesh of the entire body.

Huang et al. [108] present a new method called Human-Norm, which enhances the model’s 2D perception of 3D geometry by learning a normal-adapted diffusion model and a normal-aligned diffusion model. Additionally, it introduces a progressive geometry generation strategy and a multi-step Score Distillation Sampling (SDS) loss function to improve the performance of 3D human generation.

Stathopoulos et al. [109] present a method called ScoreHMR, aimed at addressing the problem of predicting human model parameters from 2D image evidence. The ScoreHMR method mimics model fitting procedure, where a diffusion model is trained to capture the conditional distribution of human model parameters for a given input image. By using task-specific scores to guide its denoising process, ScoreHMR effectively resolves inverse problems across various applications without the need to retrain the diffusion model for each specific task.

Xu et al. [110] introduce a new task of predicting human-object interactions (HOI) in 3D space, with the primary goal of generating long-term, diverse, and vivid 3D HOI sequences. The authors propose a framework called InterDiff, which combines interaction diffusion with physics-informed interaction correction to generate realistic and physically plausible future 3D sequences of human-object interactions.

Yuan et al. [111] introduce a novel physics-guided human motion diffusion model called PhysDiff, which addresses the issue that traditional motion diffusion models often neglect physical laws, leading to the generation of physically unrealistic motions. The model incorporates physical constraints during the diffusion process by using a physics-based motion projection module. This module employs motion imitation from a physics simulator to project the denoised motions in the diffusion steps onto physically plausible movements.

## F. Scene Generation

Scene generation focuses on constructing complete 3D environments, including objects, textures, and spatial layouts.

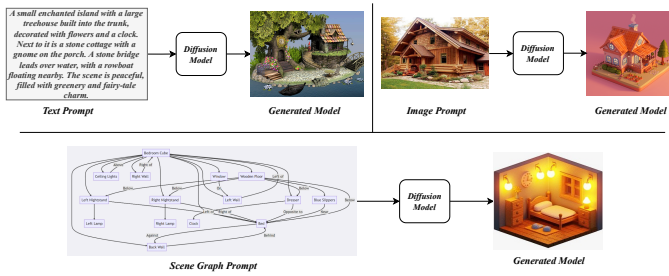


Fig. 7. Example of 3D scene generation task.

Diffusion models play a key role by learning to synthesize cohesive scenes with realistic spatial relationships between objects, lighting conditions, and textures. This has implications for virtual world creation, architectural design, and immersive experiences in gaming.

Kim et al. [112] study how to automatically generate generative models for complex open-world 3D environments. The authors first train a scene autoencoder to express image and pose pairs as a neural field. They then use a Latent Auto-Encoder to further compress the neural field representation, mapping voxel grids to a set of latent representations. Finally, they train a hierarchical diffusion model on the latent representations to complete the scene generation process.

Wynn et al. [113] address the issue that NeRF can severely restrict scene geometry and color fields when only a limited number of input views are available, which may lead to unrealistic rendering results. The authors propose a method that utilizes a Denoising Diffusion Model (DDM) as a learned prior to regularize NeRF, using the DDM to learn prior knowledge about the scene’s geometry and color. This DDM is trained on RGBD image patches from the synthetic Hypersim dataset.

Chung et al. [114] presents LucidDreamer, which maintains and expands its world model through the repeated application of two operations: "Dreaming" and "Alignment." The Dreaming process involves generating geometrically consistent images and elevating these images into 3D space. The Alignment algorithm harmoniously integrates the newly generated 3D point cloud segments into the existing 3D scene.

Fridman et al. [115] propose a novel framework that combines a pre-trained text-to-image generation model with a monocular depth prediction model, optimizing during testing to achieve online 3D-consistent scene video generation.

Wu et al. [116] introduce a method called BlockFusion, which utilizes latent 3D plane extrapolation techniques to compress 3D planes into a latent plane space using a Variational Autoencoder (VAE). In this space, a denoising diffusion process is performed to generate high-quality 3D scenes that can be infinitely scalable.

Gao et al. [117] present GraphDreamer, a framework that generates compositional 3D scenes from scene graphs. By leveraging scene graph information, it effectively addresses the issues of attribute confusion and guidance collapse in text-to-3D generation.

Ran et al. [23] introduce a new generative model called

LiDAR Diffusion Models (LiDMs), which aims to enhance the fidelity of LiDAR scenes by capturing realism through the incorporation of geometric priors. This approach improves pattern authenticity, geometric authenticity, and object authenticity, enabling the generation of LiDAR scenes that are closer to real-world data.

Tang et al. [118] propose DiffuScene, which aims to generate diverse and realistic indoor 3D scenes. DiffuScene is based on a denoising diffusion model that represents the scene as a collection of unordered objects, where each object is characterized by attributes including position, size, orientation, semantics, and geometric features. It synthesizes a 3D indoor object collection by denoising a series of unordered object attributes.

Po et al. [119] explore how to control the generation of different parts of a scene using text prompts and bounding boxes while ensuring natural transitions between these parts. The authors propose Locally Conditioned Diffusion, which allows users to control specific areas of an image through text prompts and corresponding bounding boxes.

Zhang et al. [120] present a framework called Text2NeRF, which combines text-to-image diffusion models with NeRF to generate 3D scenes with complex geometric structures and high-fidelity textures from text prompts. This method successfully enhances the realism and multi-view consistency of the generated scenes through progressive scene refinement and update strategies, as well as depth alignment strategies.

**G. 3D Editing & Manipulation**

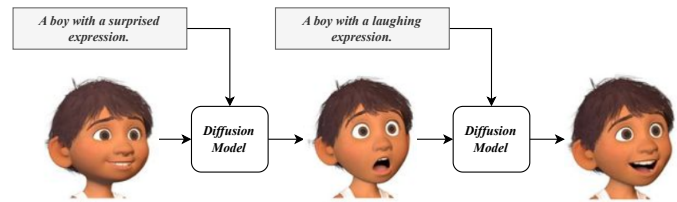


Fig. 8. Example of 3D editing task.

3D editing and manipulation refers to editing or modifying existing 3D objects or scenes. Diffusion models can be employed to make subtle adjustments to shape, texture, or pose while preserving realism. By operating directly on the 3D data or its latent representation, diffusion models allow for efficient manipulation of 3D structures with minimal distortion.

Kim et al. [121] propose DATID-3D, a novel domain adaptation method for 3D generation models. It leverages text-to-image diffusion models and adversarial training to preserve diversity in the text prompts, transforming samples from a pre-trained 3D generator into diversified target images, while generating high-quality 3D images.

Mikaeili et al. [122] presents SKED, an innovative 3D editing technique that combines sketch guidance and text prompts, breaking the problem down into two sub-tasks: the first involves coarse positioning and boundary definition based on pure geometric reasoning; the second uses the rich semantic knowledge of generative models to add and refine geometric

and texture details. By utilizing at least two guiding sketches from different viewpoints to modify existing neural fields, SKED achieves intuitive, localized, and meaningful editing of 3D shapes through a novel loss function and editing workflow.

Sella et al. [123] introduce a new technique called Vox-E, which uses text-based prompts and diffusion models to edit the voxel representation of 3D objects. It takes multi-view 2D images of a 3D object as input and learns its grid-based volumetric representation. The researchers introduce a novel volumetric regularization loss that operates directly in 3D space, leveraging the explicit nature of the 3D representation to enforce correlations between the global structure of the original and edited objects.

Han et al. [124] aim to address the issues of identity feature loss or suboptimal editing results in existing text-guided 3D head models editing. They propose a coarse-to-fine workflow called HeadSculpt, which first integrates landmark-based ControlNet and text inversion techniques to inject 3D awareness into the diffusion model, ensuring consistency of the generated head models from different viewpoints. Then, using ControlNet with InstructPix2Pix implementation, it blends editing and identity-preserving scores to optimize the texture mesh, while maintaining the original identity information and adhering to the editing instructions.

Zhuang et al. [125] propose a framework called DreamEditor, designed to control and edit the neural field representations of 3D scenes using text prompts while preserving the invariance of regions unrelated to the text prompts. By representing the scene as a grid-based neural field and leveraging a pre-trained text-to-image diffusion model to automatically identify the areas that need editing based on the semantics of the text prompt, the framework enables precise and high-quality editing of 3D scenes.

Liu et al. [126] propose SketchDream, a technique that combines sketch and text prompts, utilizing multi-view image generation and 3D editing technology to achieve high-quality generation and editing of complex 3D models from simple 2D sketches. To address the ambiguity in the 2D-to-3D conversion, they introduce a sketch-based multi-view image generation diffusion model that leverages depth information to establish spatial correspondences. A 3D ControlNet is employed to control the multi-view images and ensure their 3D consistency. To support localized editing, a coarse-to-fine editing framework is proposed. In the coarse stage, component interactions are analyzed, and a 3D mask is provided to mark the editing region; in the fine stage, local enhancement is applied to generate realistic results with fine details.

Chen et al. [127] propose GaussianEditor, aimed at addressing the limitations of traditional 3D editing methods in handling complex scenes and the shortcomings of implicit 3D NeRF-based approaches in terms of processing speed and editing control. The paper introduces Gaussian Semantic Tracing, which enables precise control over Gaussian Splatting by tracking the editing target throughout the training process. To overcome the difficulty GS faces in achieving fine results under random generation guidance, the authors propose Hierarchical Gaussian Splatting, which divides Gaussian points into different "generations" and applies varying levels of

constraints to each generation of points.

Decatur et al. [12] propose 3D Paintbrush, aimed at addressing the fundamental capability of editing existing high-quality 3D assets within the 3D modeling workflow, particularly for localized editing. Unlike previous works that primarily focus on global editing, 3D Paintbrush utilizes Cascaded Score Distillation techniques to represent local textures as neural textures defined on the surface of a mesh. This approach optimizes textures and localization maps through a Multi-Layer Perceptron (MLP), enabling text-based localized stylization of textures on 3D mesh models. This method generates richly detailed textures that closely adhere to the localized regions.

Pandey et al. [128] investigate how to perform 3D editing on images, such as 3D translation and rotation, using pre-trained diffusion models without requiring additional training or fine-tuning, while ensuring that the edited images appear plausible in terms of perspective, occlusion, lighting, and shadows. The authors propose a method that elevates the activations of the diffusion model into 3D space using proxy depth. The elevated activations are then transformed in 3D space and projected back into image space to guide the diffusion process, resulting in the generation of edited images.

Yoo et al. [129] propose APAP, aimed at enhancing the visual realism of deformed meshes during user interactive editing processes. The APAP framework uses the Jacobian matrix for each face to represent mesh deformations, calculating the vertex coordinates of the mesh through a differentiable Poisson solver. First, the deformed mesh is rendered into a 2D image, from which meaningful and reasonable priors are extracted using the SDS process. To better preserve the identity of the edited mesh, the authors fine-tune a 2D diffusion model using LoRA. Finally, the ultimate deformation is computed through iterative gradient descent, balancing user edits with output plausibility.

## H. Novel View Synthesis

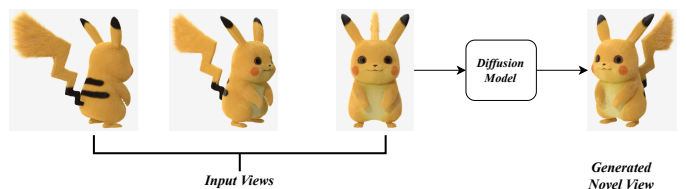


Fig. 9. Example of novel view synthesis task.

Novel view synthesis aims to generate images of a scene from unseen viewpoints based on limited input views. Diffusion models excel in this area by predicting how a scene should appear from different angles, providing consistent and coherent visual outputs. This is essential for applications in virtual tourism, interactive media, and robotics, where understanding the environment from multiple perspectives is crucial.

Deng et al. [130] propose a framework called NeRDi, which utilizes general image priors from 2D diffusion models for single-view NeRF synthesis. NeRDi formulates the single-view reconstruction problem as a 3D generation problem

constrained by image conditions, optimizing the NeRF representation by minimizing the image distribution loss of the diffusion model on rendering from arbitrary views.

Karnewar et al. [131] propose a method called HOLODIFFUSION, which employs a mixed explicit-implicit feature grid. This method adds noise only to the input 2D images and then trains a denoising 3D UNet network to remove the noise. It enables the training of a 3D perception generation diffusion model using only 2D image supervision. Additionally, since the features are defined in 3D space, images can be rendered from any desired viewpoint and maintain consistency across different viewpoints.

Tseng et al. [132] investigate the problem of generating long-term consistent and high-quality new view sequences when there is significant camera motion. They propose a pose-guided diffusion model, designing an epipolar attention layer within the network to relate the features of the input and output views. Using camera pose information, they estimate the epipolar lines on the feature maps of the input views to calculate the attention weights between the input and output views.

Zhou et al. [133] primarily focus on how to perform 3D reconstruction from a small number of segmented input images with known relative poses (e.g., two images). SparseFusion combines state-of-the-art neural rendering and probabilistic image generation techniques, utilizing a view-conditioned latent diffusion model (VLDM) to generate detailed new view images. It optimizes an instance-specific (neural) 3D representation by maximizing the likelihood of the conditional distribution modeled by the VLDM.

Liu et al. [134] investigate how to synthesize new-view 3D object images from a single RGB image in a zero-shot manner. The authors propose the Zero-1-to-3 framework, which is trained on a synthetic dataset to learn the control of relative camera viewpoints. This enables the generation of new images of the same object under specified camera transformations. Additionally, the framework incorporates a 3D reconstruction task by optimizing a neural field to achieve 3D reconstruction from a single image.

Chan et al. [135] design an NVS framework that builds upon existing 2D diffusion models, but crucially incorporates a 3D geometric prior in the form of a 3D feature volume. This latent feature field captures the distribution of potential scene representations and enhances the ability to generate new rendered images that are consistent across viewpoints.

Shi et al. [136] explore improving existing single-image-to-3D conversion techniques, addressing common issues such as texture degradation and geometric misalignment in generated images. They model the joint distribution of multiple images by stitching six views (in a 3x2 layout) into a single image. Additionally, they enhance the model’s ability to generate globally consistent images by modifying the noise schedule.

Watson et al. [137] proposes DiM, which utilizes a pose-conditioned image-to-image diffusion model. It takes a source view and its pose as input and generates a new view in the target pose as output. The authors employ a stochastic conditioning to randomly select conditional views during the generation process, improving the 3D consistency of the

generated images. Additionally, they use a novel variant of the UNet architecture specifically designed for 3D view synthesis, enhancing performance by sharing weights between the two input images and using cross-attention between the views.

Gu et al. [138] propose a method called NerfDiff, which addresses the uncertainty issues faced by existing Neural Radiance Field (NeRF) methods when handling severe occlusions by synthesizing and optimizing a set of virtual views during testing. At the core of NerfDiff is the integration of knowledge from a 3D-aware conditional diffusion model (CDM) into NeRF through a NeRF-guided distillation process.

Höllein et al. [139] propose a new method that leverages a pretrained text-to-image model as a prior. By incorporating 3D volumetric rendering, cross-frame attention layers, and an autoregressive generation strategy, the model is able to condition the generation of the next viewpoint’s image on previously generated images during the process. This approach enables the generation of high-quality images that are consistent with real-world 3D objects across multiple viewpoints, based on either text or image inputs.

Ye et al. [140] decompose the NVS task into two stages. First, use a Scene Representation Transformer to transform the observed regions to the new view, and then use a view-conditioned diffusion model to imagine the unseen regions. Additionally, they introduced a hierarchical generation paradigm capable of producing consistent long-view sequences, allowing a comprehensive 360° observation of the provided object image.

Liu et al. [141] introduce a novel diffusion model called SyncDreamer, which achieves consistent image generation in a single reverse process by modeling the joint probability distribution of multi-view images. The authors use a 3D-aware feature attention mechanism to synchronize the intermediate states of the generated images by associating corresponding features across different viewpoints. Additionally, they initialize SyncDreamer with a pretrained diffusion model to maintain strong generalization capabilities.

## 1. Depth Estimation

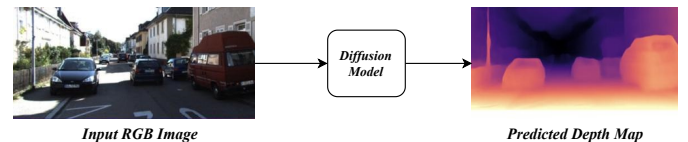


Fig. 10. Example of depth estimation task.

Depth estimation refers to estimating the depth information of a scene from input data such as 2D images or video frames. Diffusion models are utilized to progressively refine depth maps, ensuring accurate and detailed representations of scene geometry. This task is critical for applications like 3D reconstruction, augmented reality, and autonomous systems where depth perception is necessary for decision-making.

Ji et al. [142] propose DDP, a conditional diffusion model framework designed for various dense visual prediction tasks. By effectively extending the denoising diffusion process within

modern perception pipelines, DDP achieves competitive performance across multiple benchmarks without the need for task-specific designs or architectural customization. Notably, this method is one of the earliest to apply DDPMs to depth map prediction.

Li et al. [143] introduces DADP, a framework that combines diffusion models to improve depth estimation in sparsely annotated autonomous driving scenes. DADP includes a noise predictor and a depth predictor where the noise predictor enforces regional and holistic spatial structures by predicting noise components, while the depth predictor can be any single-image depth estimation model.

Zhang et al. [144] utilize Depth2Underwater ControlNet to generate a new underwater depth estimation dataset from terrestrial depth data using Stable Diffusion. This method combines the accuracy of terrestrial depth information with the realism of underwater scenes, and the dataset can be used to train underwater depth estimation models.

Patni et al. [22] propose a new monocular depth estimation model called ECoDepth, which uses a diffusion model as the backbone network. It leverages global image priors generated by a pretrained Vision Transformer (ViT) model as input to provide more detailed contextual information.

Saxena et al. [145] propose a model called DDVM, a diffusion model designed for monocular depth estimation. It combines self-supervised pretraining with supervised fine-tuning. DDVM is first pretrained on self-supervised image-to-image translation tasks, then undergoes supervised training on RGB-D data.

Ke et al. [146] introduce Marigold, a method based on stable diffusion models, which achieves state-of-the-art monocular depth estimation across multiple real-world datasets by fine-tuning on synthetic data without access to real depth samples. The authors only perform fine-tuning on the denoising U-Net, preserving the rich visual priors of the pre-trained model.

## V. 3D DATASETS AND EVALUATION METRICS

### A. 3D Datasets

In this section, we summarize some of the most commonly used datasets in current diffusion-related 3D tasks. We categorize them into three groups: object-based, human-based, and scene-based. All datasets and their details are listed in Table I.

1) **Object Datasets:** Among the various datasets available for 3D object dataset, ShapeNet [34] stands out as one of the earliest and most foundational, featuring 51K synthetic 3D CAD models across diverse categories. It has significantly influenced subsequent research in the field. CO3D [154] is notable for its large scale real scanned 3D objects, comprising 19K models, which allows for detailed analysis and has become a vital resource for fine-grained 3D object-related tasks. On the other hand, Objaverse [155] represents a major advancement in dataset size, with nearly 800K models, making it the largest among the listed datasets and facilitating extensive applications in training deep learning models for 3D understanding. In addition to the above datasets, other datasets such as ABO [152] and GSO [156] also play an important role in the research of 3D object generation.

TABLE I  
COMMONLY USED 3D DATASETS. “MS” MEANS “MESH”, “RD” MEANS “RGBD”, “PC” MEAN “POINT CLOUD”, “MV” MEANS “MULTI-VIEW”.

Name	Type	Samples	Category	Source
ShapeNet [34]	Object	51K	MS	Synth
PartNet [35]	Object	574K	MS	Synth
ModelNet40 [147]	Object	12K	MS	Synth
3dscan [148]	Object	10K	RD,PC	Real
MVP [149]	Object	100K	PC	Synth
Completion3D [150]	Object	30K	PC	Synth
PhotoShape [151]	Object	11K	MS	Synth
ABO [152]	Object	147K	MS	Synth
YCB [153]	Object	600	RD,MS	Real
CO3D [154]	Object	19K	MV	Real
Objaverse [155]	Object	800K	MS	Synth
GSO [156]	Object	1.0K	MS	Real
Cap3D [157]	Object	785k	MS	Synth
Text2Shape [158]	Object	192K	MS	Synth
3D-FUTURE [159]	Object	10K	MS	Synth
OmniObject3D [160]	Object	6K	MS,PC	Real
ScanObjectNN [161]	Object	2.9K	PC	Real
Renderpeople [162]	Human	40K	MS	Synth
THuman 2.0 [163]	Human	500	RD	Real
AzurePeople [164]	Human	56	RD	Real
HumanML3D [165]	Human	15K	MS	Synth
AMASS [166]	Human	11K	MS	Synth
HumanAct12 [167]	Human	1.2K	MS	Synth
UESTC [168]	Human	25.6K	RD	Real
FaceScape [169]	Human	18.8K	MS	Real
CustomHumans [170]	Human	600	MS	Real
CAPE [171]	Human	600	MS	Real
EMDB [172]	Human	81	RD	Real
Replica [173]	Scene	18	MS	Real
3D-FRONT [174]	Scene	19K	MS	Synth
KITTI [175]	Scene	389	RD,PC	Real
ScanNet [32]	Scene	1.5K	RD,PC	Real
S3DIS [176]	Scene	271	PC	Real
AVD [177]	Scene	20K	RD,PC	Real
LLFF [31]	Scene	32	MV	Real
DTU [14]	Scene	80	MV	Real
SceneNet [178]	Scene	57	RD	Synth
NYUdepth [30]	Scene	1.5K	RD	Real
SUN RGB-D [179]	Scene	10K	RD	Real
nuScenes [180]	Scene	1K	PC	Real
Waymo [181]	Scene	2K	PC	Real
GL3D [182]	Scene	113	MS	Real
Realestate10K [183]	Scene	750K	MV	Real
Matterport3D [184]	Scene	90	RD	Real
DDAD [185]	Scene	254	RD	Real
Hyper-sim [186]	Scene	461	MS	Synth

2) **Human Datasets:** Within those datasets focused on human representation, Renderpeople [162] is notable for being the largest synthetic dataset, comprising nearly 40K models. Its extensive scale makes it a valuable resource for various applications in computer graphics and machine learning. In contrast, the THuman 2.0 dataset [163], with 500 real human models, is recognized as one of the earliest datasets in this field, contributing significantly to research on human motion and behavior recognition. Another important dataset is UESTC [168], featuring 25.6K real human models, which stands out for its substantial size and practical applications in real-world scenarios. Other datasets, such as HumanML3D [165], AMASS [166] and FaceScape [169], also contribute important insights into human modeling and animation.

TABLE II  
METRICS AND THEIR DESCRIPTIONS.

Metric	Description
<b>Distance Metrics</b>	
CD	Measures the distance between two point sets by averaging the nearest distances between points.
EMD	Measures the minimum cost of transforming one distribution into another, treating them as mass distributions.
TMD	Evaluates the total discrepancy between two distributions over multiple dimensions.
MMD	Measures the distance between distributions by matching their elements optimally.
LFD	Quantifies the difference between light fields captured from two different perspectives.
<b>Coverage Metrics</b>	
COV	Percentage of test samples covered by generated samples.
1-NNA	Assesses how well test and generated samples are mixed based on nearest neighbors.
<b>Distribution Metrics</b>	
FID	Evaluates the similarity between two distributions by comparing their means and covariances in feature space.
FVD	Extends FID to evaluate video generation quality by comparing features extracted from video frames.
KID	Measures the distance between distributions in a feature space defined by a kernel function.
<b>Similarity Metrics</b>	
IoU	Measures the overlap between predicted and ground truth regions, commonly used in object detection.
DISTS	Evaluates the perceptual quality of images based on structural and texture similarity.
PCK	Measures the accuracy of predicted keypoints by evaluating their proximity to ground truth keypoints.
ReID	Evaluates the ability to correctly identify and match individuals across different images.
<b>Quality Metrics</b>	
PSNR	Measures the ratio between the maximum possible power of a signal and the power of corrupting noise.
SSIM	Measures the similarity between two images based on structural information, luminance, and contrast.
PF	Measures how well generated samples adhere to given prompts or instructions.
VQ	Evaluates the overall aesthetic and perceptual quality of generated images or videos.
SC	Measures the completeness of structures in generated content compared to ground truth.
PQ	Assesses the quality of generated images based on human perception and visual coherence.
<b>Error Metrics</b>	
REL	Measures the average absolute difference between predicted and true values relative to true values.
SqRel	Computes the average squared difference between predicted and true values relative to true values.
RMSE	Measures the average magnitude of the error between predicted and true values, penalizing larger errors.
RMSElog	Measures the error on a logarithmic scale to handle predictions that are orders of magnitude apart.

3) *Scene Datasets*: In those 3d scene datasets, Realestate10K [183] is notable for being the largest dataset, comprising 750K scenes, which significantly contributes to advancements in scene recognition and analysis. KITTI [175] holds the distinction of being one of the earliest datasets established for autonomous driving applications, encompassing 389 scenes and providing essential data for

research in computer vision and robotics. ScanNet [32] is recognized for its extensive real-world indoor scene collection, featuring nearly 1,500 diverse scenes, making it one of the most widely utilized datasets in training and benchmarking algorithms. Other datasets, such as NyuDepth [30] and Waymo [181], also play important roles in 3D indoor and outdoor scene-related researches.

### B. Evaluation Metrics

We categorise and list all the commonly used metrics in 3D-related tasks in Table II, including Chamfer Distance (CD), Earth Mover’s Distance (EMD), Total Mutual Difference (TMD), Minimum Matching Distance (MMD), Light Field Distance (LFD), Coverage (COV), Nearest Neighbour (1-NNA), Frechet Inception Distance (FID), Frechet Video Distance (FVD), Kernel Inception Distance (KID), Intersection over Union (IoU), Deep Image Structure and Texture Similarity (DISTS), Percentage of Correct Keypoints (PCK), Reidentification Score (ReID), Peak Signal-to-Noise Ratio (PSNR), Structural Similarity Index (SSIM), Prompt Fidelity (PF), Visual Quality (VQ), Structure Completeness (SC), Perceptual Quality (PQ), Mean Absolute Relative Error (REL), Mean Squared Relative Error (SqRel), Root Mean Squared Error (RMSE), Root Mean Squared Log Error (RMSElog).

## VI. LIMITATIONS AND FUTURE DIRECTIONS

**Improving Computational Efficiency and Inference Speed.** While diffusion models have shown great promise in generating high-quality 3D data, their computational demands remain a significant challenge. These models typically require a large number of iterations to produce results, which increases both training time and inference speed. This problem becomes more acute when working with high-dimensional 3D data, where memory and computational requirements scale rapidly. Future research could focus on optimizing the number of diffusion steps or exploring more efficient architectures, such as using denoising autoencoders or neural ordinary differential equations (ODEs), to accelerate inference without sacrificing output quality. Additionally, parallelization techniques or hardware acceleration (e.g., leveraging GPUs or TPUs) could further mitigate the computational burden.

**Multimodal Fusion.** A key challenge in 3D vision tasks is effectively integrating different data modalities, such as 2D images, 3D geometry, and textual descriptions. While diffusion models have been applied successfully to single-modality tasks, there is still room for improvement in multimodal fusion. Future work could explore methods for better combining these modalities within the diffusion framework. For instance, employing cross-attention mechanisms or utilizing embeddings that capture the relationships between 2D, 3D, and textual inputs could enhance the model’s ability to synthesize richer, more context-aware 3D content. Additionally, developing unified architectures capable of jointly handling multiple modalities could broaden the application of diffusion models in tasks such as 3D scene generation and object understanding.

**Large-scale Pretraining and Transfer Learning.** Large-scale pretraining has been pivotal in achieving state-of-the-art results in many 2D vision tasks, yet its application in

3D diffusion models remains underexplored. Pretraining 3D diffusion models on vast datasets, followed by fine-tuning on specific downstream tasks, could help mitigate the need for large annotated 3D datasets. Furthermore, effective transfer learning techniques could be developed to allow pretrained models to generalize across diverse 3D tasks, such as reconstruction, generation, and recognition. Identifying robust pretraining strategies and understanding the transferability of knowledge across 2D and 3D domains are promising areas for future research.

**Interpretability and Control.** One of the major limitations of current diffusion models is the lack of interpretability and fine-grained control over the generation process. This issue is particularly relevant in 3D vision, where users may want to influence specific aspects of the generated 3D content, such as shape, texture, or pose. Future work should focus on enhancing the transparency of these models by developing interpretable latent spaces or integrating control mechanisms. Techniques such as latent space manipulation, conditional generation, or disentanglement of various attributes could empower users to direct the output in more predictable ways. Moreover, explainability tools could help users understand how the model arrives at specific outputs, increasing trust and usability in real-world applications.

**Application to Complex and Dynamic Scenes.** Current diffusion models in 3D vision are mostly applied to static objects or scenes, but extending them to handle complex and dynamic environments remains a key challenge. Real-world 3D scenes often involve dynamic elements such as moving objects, changing lighting conditions, or large-scale outdoor environments. To address these complexities, future research should explore methods for encoding temporal information and handling dynamic changes within diffusion models. This could involve the integration of spatiotemporal diffusion processes or the development of hybrid models that combine static scene understanding with temporal dynamics. Successfully extending these models to dynamic and large-scale 3D environments would open up new possibilities for applications in simulation, virtual reality, and robotics.

**Incorporation of Physical Constraints.** Incorporating physical constraints into 3D diffusion models is crucial for generating realistic and plausible 3D content. Future research could focus on integrating principles from physics, such as conservation laws, collision detection, and material properties, to ensure that generated 3D objects behave in accordance with the real world. This could involve embedding physics-based priors or loss functions into the training process to encourage physically accurate outputs. For example, enforcing geometric consistency or simulating real-world interactions, such as gravity or fluid dynamics, could enhance the realism of the generated 3D content. By grounding these models in physical laws, they could be more effectively applied in engineering, simulation, and other fields where physical accuracy is paramount.

## VII. CONCLUSION

In this paper, we presented a comprehensive survey on the application of diffusion models to 3D vision tasks. We

explored how these models, originally designed for 2D generative tasks, have been adapted to handle the complexities of 3D data, such as point clouds, meshes, and voxel grids. We reviewed key approaches that apply diffusion models to tasks like 3D object generation, shape completion, point cloud reconstruction, and scene generation. We provided an in-depth discussion of the underlying mathematical principles of diffusion models, outlining their forward and reverse processes, as well as the various architectural advancements that enable these models to work with 3D data. Additionally, we categorized and analyzed the different 3D tasks where diffusion models have shown significant impact, such as text-to-3D generation, mesh generation, and novel view synthesis. The paper also addressed the key challenges in applying diffusion models to 3D vision, such as handling occlusions, varying point densities, and the computational demands of high-dimensional data. To guide future research, we discussed potential solutions, including improving computational efficiency, enhancing multimodal fusion, and exploring the use of large-scale pretraining for better generalization across 3D tasks. By consolidating the current state of diffusion models in 3D vision and identifying gaps and opportunities, this paper serves as a foundation for future exploration and development in this rapidly evolving field.

## REFERENCES

- [1] J. Ho, A. Jain, and P. Abbeel, "Denoising diffusion probabilistic models," *Advances in neural information processing systems*, vol. 33, pp. 6840–6851, 2020.
- [2] Y. Song and S. Ermon, "Improved techniques for training score-based generative models," *Advances in neural information processing systems*, vol. 33, pp. 12 438–12 448, 2020.
- [3] Y. Song, J. Sohl-Dickstein, D. P. Kingma, A. Kumar, S. Ermon, and B. Poole, "Score-based generative modeling through stochastic differential equations," in *International Conference on Learning Representations*, 2021.
- [4] A. Q. Nichol and P. Dhariwal, "Improved denoising diffusion probabilistic models," in *International conference on machine learning*. PMLR, 2021, pp. 8162–8171.
- [5] D. Watson, W. Chan, J. Ho, and M. Norouzi, "Learning fast samplers for diffusion models by differentiating through sample quality," in *International Conference on Learning Representations*, 2022.
- [6] P. Dhariwal and A. Nichol, "Diffusion models beat gans on image synthesis," *Advances in neural information processing systems*, vol. 34, pp. 8780–8794, 2021.
- [7] R. Rombach, A. Blattmann, D. Lorenz, P. Esser, and B. Ommer, "High-resolution image synthesis with latent diffusion models," in *Proceedings of the IEEE/CVF conference on computer vision and pattern recognition*, 2022, pp. 10 684–10 695.
- [8] C. Saharia, W. Chan, S. Saxena, L. Li, J. Whang, E. L. Denton, K. Ghasemipour, R. Gontijo Lopes, B. Karagol Ayan, T. Salimans *et al.*, "Photorealistic text-to-image diffusion models with deep language understanding," *Advances in neural information processing systems*, vol. 35, pp. 36 479–36 494, 2022.
- [9] A. Q. Nichol, P. Dhariwal, A. Ramesh, P. Shyam, P. Mishkin, B. McGrew, I. Sutskever, and M. Chen, "Glide: Towards photorealistic image generation and editing with text-guided diffusion models," in *International Conference on Machine Learning*. PMLR, 2022, pp. 16 784–16 804.
- [10] V. Kulikov, S. Yadin, M. Kleiner, and T. Michaeli, "Sinddm: A single image denoising diffusion model," in *International conference on machine learning*. PMLR, 2023, pp. 17 920–17 930.
- [11] B. Xia, Y. Zhang, S. Wang, Y. Wang, X. Wu, Y. Tian, W. Yang, and L. Van Gool, "Diffir: Efficient diffusion model for image restoration," in *Proceedings of the IEEE/CVF International Conference on Computer Vision*, 2023, pp. 13 095–13 105.

- [12] D. DeCATUR, I. Lang, K. Aberman, and R. Hanocka, “3d paintbrush: Local stylization of 3d shapes with cascaded score distillation,” in *Proceedings of the IEEE/CVF Conference on Computer Vision and Pattern Recognition*, 2024, pp. 4473–4483.
- [13] J. Shim, C. Kang, and K. Joo, “Diffusion-based signed distance fields for 3d shape generation,” in *Proceedings of the IEEE/CVF conference on computer vision and pattern recognition*, 2023, pp. 20 887–20 897.
- [14] R. Jensen, A. Dahl, G. Vogiatzis, E. Tola, and H. Aanæs, “Large scale multi-view stereopsis evaluation,” in *Proceedings of the IEEE conference on computer vision and pattern recognition*, 2014, pp. 406–413.
- [15] L. Zhou, Y. Du, and J. Wu, “3d shape generation and completion through point-voxel diffusion,” in *Proceedings of the IEEE/CVF international conference on computer vision*, 2021, pp. 5826–5835.
- [16] Z. Ren, M. Kim, F. Liu, and X. Liu, “Tiger: Time-varying denoising model for 3d point cloud generation with diffusion process,” in *Proceedings of the IEEE/CVF Conference on Computer Vision and Pattern Recognition*, 2024, pp. 9462–9471.
- [17] S. Mo, E. Xie, R. Chu, L. Hong, M. Niessner, and Z. Li, “Dit-3d: Exploring plain diffusion transformers for 3d shape generation,” *Advances in neural information processing systems*, vol. 36, pp. 67 960–67 971, 2023.
- [18] G. Chou, Y. Bahat, and F. Heide, “Diffusion-sdf: Conditional generative modeling of signed distance functions,” in *Proceedings of the IEEE/CVF international conference on computer vision*, 2023, pp. 2262–2272.
- [19] Z. Lyu, Z. Kong, X. Xudong, L. Pan, and D. Lin, “A conditional point diffusion-refinement paradigm for 3d point cloud completion,” in *International Conference on Learning Representations*, 2022.
- [20] L. Nunes, R. Marcuzzi, B. Mersch, J. Behley, and C. Stachniss, “Scaling diffusion models to real-world 3d lidar scene completion,” in *Proceedings of the IEEE/CVF Conference on Computer Vision and Pattern Recognition*, 2024, pp. 14 770–14 780.
- [21] B. Zhang, J. Tang, M. Niessner, and P. Wonka, “3dshape2vecset: A 3d shape representation for neural fields and generative diffusion models,” *ACM Transactions on Graphics (TOG)*, vol. 42, no. 4, pp. 1–16, 2023.
- [22] S. Patni, A. Agarwal, and C. Arora, “Ecodepth: Effective conditioning of diffusion models for monocular depth estimation,” in *Proceedings of the IEEE/CVF Conference on Computer Vision and Pattern Recognition*, 2024, pp. 28 285–28 295.
- [23] H. Ran, V. Guizilini, and Y. Wang, “Towards realistic scene generation with lidar diffusion models,” in *Proceedings of the IEEE/CVF Conference on Computer Vision and Pattern Recognition*, 2024, pp. 14 738–14 748.
- [24] S. R. De Groot and P. Mazur, *Non-equilibrium thermodynamics*. Courier Corporation, 2013.
- [25] J. Sohl-Dickstein, E. Weiss, N. Maheswaranathan, and S. Ganguli, “Deep unsupervised learning using nonequilibrium thermodynamics,” in *International conference on machine learning*. PMLR, 2015, pp. 2256–2265.
- [26] N. Ikeda and S. Watanabe, *Stochastic differential equations and diffusion processes*. Elsevier, 2014.
- [27] L. Zhang, A. Rao, and M. Agrawala, “Adding conditional control to text-to-image diffusion models,” in *Proceedings of the IEEE/CVF International Conference on Computer Vision*, 2023, pp. 3836–3847.
- [28] I. Goodfellow, J. Pouget-Abadie, M. Mirza, B. Xu, D. Warde-Farley, S. Ozair, A. Courville, and Y. Bengio, “Generative adversarial networks,” *Communications of the ACM*, vol. 63, no. 11, pp. 139–144, 2020.
- [29] D. P. Kingma, “Auto-encoding variational bayes,” *arXiv preprint arXiv:1312.6114*, 2013.
- [30] N. Silberman, D. Hoiem, P. Kohli, and R. Fergus, “Indoor segmentation and support inference from rgb-d images,” in *Computer Vision—ECCV 2012: 12th European Conference on Computer Vision, Florence, Italy, October 7-13, 2012, Proceedings, Part V 12*. Springer, 2012, pp. 746–760.
- [31] B. Mildenhall, P. P. Srinivasan, R. Ortiz-Cayon, N. K. Kalantari, R. Ramamoorthi, R. Ng, and A. Kar, “Local light field fusion: Practical view synthesis with prescriptive sampling guidelines,” *ACM Transactions on Graphics (ToG)*, vol. 38, no. 4, pp. 1–14, 2019.
- [32] A. Dai, A. X. Chang, M. Savva, M. Halber, T. Funkhouser, and M. Nießner, “Scannet: Richly-annotated 3d reconstructions of indoor scenes,” in *Proceedings of the IEEE conference on computer vision and pattern recognition*, 2017, pp. 5828–5839.
- [33] Y. Zhou and O. Tuzel, “Voxelnet: End-to-end learning for point cloud based 3d object detection,” in *Proceedings of the IEEE conference on computer vision and pattern recognition*, 2018, pp. 4490–4499.
- [34] A. X. Chang, T. Funkhouser, L. Guibas, P. Hanrahan, Q. Huang, Z. Li, S. Savarese, M. Savva, S. Song, H. Su *et al.*, “Shapenet: An information-rich 3d model repository,” *arXiv preprint arXiv:1512.03012*, 2015.
- [35] K. Mo, S. Zhu, A. X. Chang, L. Yi, S. Tripathi, L. J. Guibas, and H. Su, “Partnet: A large-scale benchmark for fine-grained and hierarchical part-level 3d object understanding,” in *Proceedings of the IEEE/CVF conference on computer vision and pattern recognition*, 2019, pp. 909–918.
- [36] B. Mildenhall, P. P. Srinivasan, M. Tancik, J. T. Barron, R. Ramamoorthi, and R. Ng, “Nerf: Representing scenes as neural radiance fields for view synthesis,” *Communications of the ACM*, vol. 65, no. 1, pp. 99–106, 2021.
- [37] X. Xu, X. Pan, D. Lin, and B. Dai, “Generative occupancy fields for 3d surface-aware image synthesis,” *Advances in Neural Information Processing Systems*, vol. 34, pp. 20 683–20 695, 2021.
- [38] H. Oleynikova, Z. Taylor, M. Fehr, R. Siegwart, and J. Nieto, “Voxblox: Incremental 3d euclidean signed distance fields for on-board map planning,” in *2017 IEEE/RSJ International Conference on Intelligent Robots and Systems (IROS)*. IEEE, 2017, pp. 1366–1373.
- [39] B. Kerbl, G. Kopanas, T. Leimkühler, and G. Drettakis, “3d gaussian splatting for real-time radiance field rendering,” *ACM Trans. Graph.*, vol. 42, no. 4, pp. 139–1, 2023.
- [40] K. Hara, H. Kataoka, and Y. Satoh, “Can spatiotemporal 3d cnns retrace the history of 2d cnns and imagenet?” in *Proceedings of the IEEE conference on Computer Vision and Pattern Recognition*, 2018, pp. 6546–6555.
- [41] C. R. Qi, H. Su, K. Mo, and L. J. Guibas, “Pointnet: Deep learning on point sets for 3d classification and segmentation,” in *Proceedings of the IEEE conference on computer vision and pattern recognition*, 2017, pp. 652–660.
- [42] C. R. Qi, L. Yi, H. Su, and L. J. Guibas, “Pointnet++: Deep hierarchical feature learning on point sets in a metric space,” *Advances in neural information processing systems*, vol. 30, 2017.
- [43] J. Zhou, G. Cui, S. Hu, Z. Zhang, C. Yang, Z. Liu, L. Wang, C. Li, and M. Sun, “Graph neural networks: A review of methods and applications,” *AI open*, vol. 1, pp. 57–81, 2020.
- [44] L. Mescheder, M. Oechsle, M. Niemeyer, S. Nowozin, and A. Geiger, “Occupancy networks: Learning 3d reconstruction in function space,” in *Proceedings of the IEEE/CVF conference on computer vision and pattern recognition*, 2019, pp. 4460–4470.
- [45] J. J. Park, P. Florence, J. Straub, R. Newcombe, and S. Lovegrove, “Deepsdf: Learning continuous signed distance functions for shape representation,” in *Proceedings of the IEEE/CVF conference on computer vision and pattern recognition*, 2019, pp. 165–174.
- [46] A. Vaswani, “Attention is all you need,” *Advances in Neural Information Processing Systems*, 2017.
- [47] H. Zhao, L. Jiang, J. Jia, P. H. Torr, and V. Koltun, “Point transformer,” in *Proceedings of the IEEE/CVF international conference on computer vision*, 2021, pp. 16 259–16 268.
- [48] I. Misra, R. Girdhar, and A. Joulin, “An end-to-end transformer model for 3d object detection,” in *Proceedings of the IEEE/CVF international conference on computer vision*, 2021, pp. 2906–2917.
- [49] X. Zheng, X. Huang, G. Mei, Y. Hou, Z. Lyu, B. Dai, W. Ouyang, and Y. Gong, “Point cloud pre-training with diffusion models,” in *Proceedings of the IEEE/CVF Conference on Computer Vision and Pattern Recognition*, 2024, pp. 22 935–22 945.
- [50] N. Müller, Y. Siddiqui, L. Porzi, S. R. Buló, P. Kotschieder, and M. Nießner, “Diffrr: Rendering-guided 3d radiance field diffusion,” in *Proceedings of the IEEE/CVF Conference on Computer Vision and Pattern Recognition*, 2023, pp. 4328–4338.
- [51] J. R. Shue, E. R. Chan, R. Po, Z. Ankner, J. Wu, and G. Wetzstein, “3d neural field generation using triplane diffusion,” in *Proceedings of the IEEE/CVF Conference on Computer Vision and Pattern Recognition*, 2023, pp. 20 875–20 886.
- [52] J. Koo, S. Yoo, M. H. Nguyen, and M. Sung, “Salad: Part-level latent diffusion for 3d shape generation and manipulation,” in *Proceedings of the IEEE/CVF International Conference on Computer Vision*, 2023, pp. 14 441–14 451.
- [53] G. Nam, M. Khelifi, A. Rodriguez, A. Tono, L. Zhou, and P. Guerrero, “3d-ldm: Neural implicit 3d shape generation with latent diffusion models,” *arXiv preprint arXiv:2212.00842*, 2022.
- [54] A. Vahdat, F. Williams, Z. Gojcic, O. Litany, S. Fidler, K. Kreis *et al.*, “Lion: Latent point diffusion models for 3d shape generation,” *Advances in Neural Information Processing Systems*, vol. 35, pp. 10 021–10 039, 2022.

- [55] Y. Kasten, O. Rahamim, and G. Chechik, "Point cloud completion with pretrained text-to-image diffusion models," *Advances in Neural Information Processing Systems*, vol. 36, 2024.
- [56] H. Wang, X. Du, J. Li, R. A. Yeh, and G. Shakhnarovich, "Score jacobian chaining: Lifting pretrained 2d diffusion models for 3d generation," in *Proceedings of the IEEE/CVF Conference on Computer Vision and Pattern Recognition*, 2023, pp. 12 619–12 629.
- [57] D. Xu, Y. Jiang, P. Wang, Z. Fan, Y. Wang, and Z. Wang, "Neurallift-360: Lifting an in-the-wild 2d photo to a 3d object with 360deg views," in *Proceedings of the IEEE/CVF Conference on Computer Vision and Pattern Recognition*, 2023, pp. 4479–4489.
- [58] S. Szymanowicz, C. Rupprecht, and A. Vedaldi, "Viewset diffusion:(0-) image-conditioned 3d generative models from 2d data," in *Proceedings of the IEEE/CVF International Conference on Computer Vision*, 2023, pp. 8863–8873.
- [59] L. Melas-Kyriazi, I. Laina, C. Rupprecht, and A. Vedaldi, "Realfusion: 360deg reconstruction of any object from a single image," in *Proceedings of the IEEE/CVF conference on computer vision and pattern recognition*, 2023, pp. 8446–8455.
- [60] M. Liu, C. Xu, H. Jin, L. Chen, M. Varma, T. Z. Xu, and H. Su, "One-2-3-45: Any single image to 3d mesh in 45 seconds without per-shape optimization," *Advances in Neural Information Processing Systems*, vol. 36, 2024.
- [61] M. Liu, R. Shi, L. Chen, Z. Zhang, C. Xu, X. Wei, H. Chen, C. Zeng, J. Gu, and H. Su, "One-2-3-45++: Fast single image to 3d objects with consistent multi-view generation and 3d diffusion," in *Proceedings of the IEEE/CVF Conference on Computer Vision and Pattern Recognition*, 2024, pp. 10 072–10 083.
- [62] Z. Hu, M. Zhao, C. Zhao, X. Liang, L. Li, Z. Zhao, C. Fan, X. Zhou, and X. Yu, "Efficientdreamer: High-fidelity and robust 3d creation via orthogonal-view diffusion priors," in *Proceedings of the IEEE/CVF Conference on Computer Vision and Pattern Recognition*, 2024, pp. 4949–4958.
- [63] X. Long, Y.-C. Guo, C. Lin, Y. Liu, Z. Dou, L. Liu, Y. Ma, S.-H. Zhang, M. Habermann, C. Theobalt *et al.*, "Wonder3d: Single image to 3d using cross-domain diffusion," in *Proceedings of the IEEE/CVF Conference on Computer Vision and Pattern Recognition*, 2024, pp. 9970–9980.
- [64] J. Tang, T. Wang, B. Zhang, T. Zhang, R. Yi, L. Ma, and D. Chen, "Make-it-3d: High-fidelity 3d creation from a single image with diffusion prior," in *Proceedings of the IEEE/CVF international conference on computer vision*, 2023, pp. 22 819–22 829.
- [65] X.-Y. Zheng, H. Pan, P.-S. Wang, X. Tong, Y. Liu, and H.-Y. Shum, "Locally attentional sdf diffusion for controllable 3d shape generation," *ACM Transactions on Graphics (ToG)*, vol. 42, no. 4, pp. 1–13, 2023.
- [66] Y. Lin, H. Han, C. Gong, Z. Xu, Y. Zhang, and X. Li, "Consistent123: One image to highly consistent 3d asset using case-aware diffusion priors," *arXiv preprint arXiv:2309.17261*, 2023.
- [67] G. Qian, J. Mai, A. Hamdi, J. Ren, A. Siarohin, B. Li, H.-Y. Lee, I. Skorokhodov, P. Wonka, S. Tulyakov *et al.*, "Magic123: One image to high-quality 3d object generation using both 2d and 3d diffusion priors," *arXiv preprint arXiv:2306.17843*, 2023.
- [68] J. Tang, Z. Chen, X. Chen, T. Wang, G. Zeng, and Z. Liu, "Lgm: Large multi-view gaussian model for high-resolution 3d content creation," *arXiv preprint arXiv:2402.05054*, 2024.
- [69] Y. Xu, Z. Shi, W. Yifan, H. Chen, C. Yang, S. Peng, Y. Shen, and G. Wetzstein, "Grm: Large gaussian reconstruction model for efficient 3d reconstruction and generation," *arXiv preprint arXiv:2403.14621*, 2024.
- [70] J. Xu, W. Cheng, Y. Gao, X. Wang, S. Gao, and Y. Shan, "Instantmesh: Efficient 3d mesh generation from a single image with sparse-view large reconstruction models," *arXiv preprint arXiv:2404.07191*, 2024.
- [71] Z. Liu, Y. Feng, M. J. Black, D. Nowrouzezahrai, L. Paull, and W. Liu, "Meshdiffusion: Score-based generative 3d mesh modeling," *arXiv preprint arXiv:2303.08133*, 2023.
- [72] A. Nichol, H. Jun, P. Dhariwal, P. Mishkin, and M. Chen, "Point-e: A system for generating 3d point clouds from complex prompts," *arXiv preprint arXiv:2212.08751*, 2022.
- [73] M. Li, Y. Duan, J. Zhou, and J. Lu, "Diffusion-sdf: Text-to-shape via voxelized diffusion," in *Proceedings of the IEEE/CVF conference on computer vision and pattern recognition*, 2023, pp. 12 642–12 651.
- [74] G. Metzger, E. Richardson, O. Patashnik, R. Giryes, and D. Cohen-Or, "Latent-nerf for shape-guided generation of 3d shapes and textures," in *Proceedings of the IEEE/CVF Conference on Computer Vision and Pattern Recognition*, 2023, pp. 12 663–12 673.
- [75] R. Chen, Y. Chen, N. Jiao, and K. Jia, "Fantasia3d: Disentangling geometry and appearance for high-quality text-to-3d content creation," in *Proceedings of the IEEE/CVF international conference on computer vision*, 2023, pp. 22 246–22 256.
- [76] Z. Wu, Y. Wang, M. Feng, H. Xie, and A. Mian, "Sketch and text guided diffusion model for colored point cloud generation," in *Proceedings of the IEEE/CVF International Conference on Computer Vision*, 2023, pp. 8929–8939.
- [77] B. Poole, A. Jain, J. T. Barron, and B. Mildenhall, "Dreamfusion: Text-to-3d using 2d diffusion," in *The Eleventh International Conference on Learning Representations*, 2023.
- [78] Y. Lu, J. Zhang, S. Li, T. Fang, D. McKinnon, Y. Tsing, L. Quan, X. Cao, and Y. Yao, "Direct2. 5: Diverse text-to-3d generation via multi-view 2.5 d diffusion," in *Proceedings of the IEEE/CVF Conference on Computer Vision and Pattern Recognition*, 2024, pp. 8744–8753.
- [79] J. Seo, W. Jang, M.-S. Kwak, H. Kim, J. Ko, J. Kim, J.-H. Kim, J. Lee, and S. Kim, "Let 2d diffusion model know 3d-consistency for robust text-to-3d generation," in *The Twelfth International Conference on Learning Representations*, 2024.
- [80] Z. Wang, C. Lu, Y. Wang, F. Bao, C. Li, H. Su, and J. Zhu, "Prolificdreamer: High-fidelity and diverse text-to-3d generation with variational score distillation," *Advances in Neural Information Processing Systems*, vol. 36, 2024.
- [81] S. Bahmani, I. Skorokhodov, V. Rong, G. Wetzstein, L. Guibas, P. Wonka, S. Tulyakov, J. J. Park, A. Tagliasacchi, and D. B. Lindell, "4d-fy: Text-to-4d generation using hybrid score distillation sampling," in *Proceedings of the IEEE/CVF Conference on Computer Vision and Pattern Recognition*, 2024, pp. 7996–8006.
- [82] Y. Huang, J. Wang, Y. Shi, B. Tang, X. Qi, and L. Zhang, "Dreamtime: An improved optimization strategy for diffusion-guided 3d generation," in *The Twelfth International Conference on Learning Representations*, 2023.
- [83] Z. Chen, F. Wang, Y. Wang, and H. Liu, "Text-to-3d using gaussian splatting," in *Proceedings of the IEEE/CVF Conference on Computer Vision and Pattern Recognition*, 2024, pp. 21 401–21 412.
- [84] H. Ling, S. W. Kim, A. Torralba, S. Fidler, and K. Kreis, "Align your gaussians: Text-to-4d with dynamic 3d gaussians and composed diffusion models," in *Proceedings of the IEEE/CVF Conference on Computer Vision and Pattern Recognition*, 2024, pp. 8576–8588.
- [85] T. Yi, J. Fang, J. Wang, G. Wu, L. Xie, X. Zhang, W. Liu, Q. Tian, and X. Wang, "Gaussiandreamer: Fast generation from text to 3d gaussians by bridging 2d and 3d diffusion models," in *Proceedings of the IEEE/CVF Conference on Computer Vision and Pattern Recognition*, 2024, pp. 6796–6807.
- [86] T. Cao, K. Kreis, S. Fidler, N. Sharp, and K. Yin, "Texfusion: Synthesizing 3d textures with text-guided image diffusion models," in *Proceedings of the IEEE/CVF International Conference on Computer Vision*, 2023, pp. 4169–4181.
- [87] D. Z. Chen, Y. Siddiqui, H.-Y. Lee, S. Tulyakov, and M. Nießner, "Text2tex: Text-driven texture synthesis via diffusion models," in *Proceedings of the IEEE/CVF International Conference on Computer Vision*, 2023, pp. 18 558–18 568.
- [88] X. Yu, P. Dai, W. Li, L. Ma, Z. Liu, and X. Qi, "Texture generation on 3d meshes with point-uv diffusion," in *Proceedings of the IEEE/CVF International Conference on Computer Vision*, 2023, pp. 4206–4216.
- [89] A. Gupta, W. Xiong, Y. Nie, I. Jones, and B. Oğuz, "3dgen: Tri-plane latent diffusion for textured mesh generation," *arXiv preprint arXiv:2303.05371*, 2023.
- [90] E. Richardson, G. Metzger, Y. Alaluf, R. Giryes, and D. Cohen-Or, "Texture: Text-guided texturing of 3d shapes," in *ACM SIGGRAPH 2023 conference proceedings*, 2023, pp. 1–11.
- [91] D. Z. Chen, H. Li, H.-Y. Lee, S. Tulyakov, and M. Nießner, "Scenetex: High-quality texture synthesis for indoor scenes via diffusion priors," in *Proceedings of the IEEE/CVF Conference on Computer Vision and Pattern Recognition*, 2024, pp. 21 081–21 091.
- [92] H. Li, Y. Feng, S. Xue, X. Liu, B. Zeng, S. Li, B. Liu, J. Liu, S. Han, and B. Zhang, "Uv-idm: Identity-conditioned latent diffusion model for face uv-texture generation," in *Proceedings of the IEEE/CVF Conference on Computer Vision and Pattern Recognition*, 2024, pp. 10 585–10 595.
- [93] Y.-Y. Yeh, J.-B. Huang, C. Kim, L. Xiao, T. Nguyen-Phuoc, N. Khan, C. Zhang, M. Chandraker, C. S. Marshall, Z. Dong *et al.*, "Texturedreamer: Image-guided texture synthesis through geometry-aware diffusion," in *Proceedings of the IEEE/CVF Conference on Computer Vision and Pattern Recognition*, 2024, pp. 4304–4314.
- [94] X. Zeng, X. Chen, Z. Qi, W. Liu, Z. Zhao, Z. Wang, B. Fu, Y. Liu, and G. Yu, "Paint3d: Paint anything 3d with lighting-less texture diffusion models," in *Proceedings of the IEEE/CVF Conference on Computer Vision and Pattern Recognition*, 2024, pp. 4252–4262.

- [95] Z. Wang, Y. Wang, Y. Chen, C. Xiang, S. Chen, D. Yu, C. Li, H. Su, and J. Zhu, "Crm: Single image to 3d textured mesh with convolutional reconstruction model," *arXiv preprint arXiv:2403.05034*, 2024.
- [96] H. Zhang, Z. Pan, C. Zhang, L. Zhu, and X. Gao, "Texpainter: Generative mesh texturing with multi-view consistency," in *ACM SIGGRAPH 2024 Conference Papers*, 2024, pp. 1–11.
- [97] Y. Zhang, Y. Liu, Z. Xie, L. Yang, Z. Liu, M. Yang, R. Zhang, Q. Kou, C. Lin, W. Wang *et al.*, "Dreammat: High-quality pbr material generation with geometry-and light-aware diffusion models," *ACM Transactions on Graphics (TOG)*, vol. 43, no. 4, pp. 1–18, 2024.
- [98] T. Wang, B. Zhang, T. Zhang, S. Gu, J. Bao, T. Baltrusaitis, J. Shen, D. Chen, F. Wen, Q. Chen *et al.*, "Rodin: A generative model for sculpting 3d digital avatars using diffusion," in *Proceedings of the IEEE/CVF conference on computer vision and pattern recognition*, 2023, pp. 4563–4573.
- [99] R. Jiang, C. Wang, J. Zhang, M. Chai, M. He, D. Chen, and J. Liao, "Avatarcraft: Transforming text into neural human avatars with parameterized shape and pose control," in *Proceedings of the IEEE/CVF International Conference on Computer Vision*, 2023, pp. 14 371–14 382.
- [100] X. Chen, M. Mihajlovic, S. Wang, S. Prokudin, and S. Tang, "Morphable diffusion: 3d-consistent diffusion for single-image avatar creation," in *Proceedings of the IEEE/CVF Conference on Computer Vision and Pattern Recognition*, 2024, pp. 10 359–10 370.
- [101] B. Lei, K. Yu, M. Feng, M. Cui, and X. Xie, "Diffusiongan3d: Boosting text-guided 3d generation and domain adaptation by combining 3d gans and diffusion priors," in *Proceedings of the IEEE/CVF Conference on Computer Vision and Pattern Recognition*, 2024, pp. 10 487–10 497.
- [102] M. Zhou, R. Hyder, Z. Xuan, and G. Qi, "Ultravatar: A realistic animatable 3d avatar diffusion model with authenticity guided textures," in *Proceedings of the IEEE/CVF Conference on Computer Vision and Pattern Recognition*, 2024, pp. 1238–1248.
- [103] Z. Chen, F. Hong, H. Mei, G. Wang, L. Yang, and Z. Liu, "Primd-iffusion: Volumetric primitives diffusion for 3d human generation," *Advances in Neural Information Processing Systems*, vol. 36, pp. 13 664–13 677, 2023.
- [104] B. Kim, P. Kwon, K. Lee, M. Lee, S. Han, D. Kim, and H. Joo, "Chupa: Carving 3d clothed humans from skinned shape priors using 2d diffusion probabilistic models," in *Proceedings of the IEEE/CVF International Conference on Computer Vision*, 2023, pp. 15 965–15 976.
- [105] D. Svitov, D. Gudkov, R. Bashirov, and V. Lempitsky, "Dinar: Diffusion inpainting of neural textures for one-shot human avatars," in *Proceedings of the IEEE/CVF International Conference on Computer Vision*, 2023, pp. 7062–7072.
- [106] N. Kolotouros, T. Alldieck, A. Zanfir, E. Bazavan, M. Fieraru, and C. Sminchisescu, "Dreamhuman: Animatable 3d avatars from text," *Advances in Neural Information Processing Systems*, vol. 36, 2024.
- [107] I. Ho, J. Song, O. Hilliges *et al.*, "Sith: Single-view textured human reconstruction with image-conditioned diffusion," in *Proceedings of the IEEE/CVF Conference on Computer Vision and Pattern Recognition*, 2024, pp. 538–549.
- [108] X. Huang, R. Shao, Q. Zhang, H. Zhang, Y. Feng, Y. Liu, and Q. Wang, "Humannorm: Learning normal diffusion model for high-quality and realistic 3d human generation," in *Proceedings of the IEEE/CVF Conference on Computer Vision and Pattern Recognition*, 2024, pp. 4568–4577.
- [109] A. Stathopoulos, L. Han, and D. Metaxas, "Score-guided diffusion for 3d human recovery," in *Proceedings of the IEEE/CVF Conference on Computer Vision and Pattern Recognition*, 2024, pp. 906–915.
- [110] S. Xu, Z. Li, Y.-X. Wang, and L.-Y. Gui, "Interdiff: Generating 3d human-object interactions with physics-informed diffusion," in *Proceedings of the IEEE/CVF International Conference on Computer Vision*, 2023, pp. 14 928–14 940.
- [111] Y. Yuan, J. Song, U. Iqbal, A. Vahdat, and J. Kautz, "Physdiff: Physics-guided human motion diffusion model," in *Proceedings of the IEEE/CVF international conference on computer vision*, 2023, pp. 16 010–16 021.
- [112] S. W. Kim, B. Brown, K. Yin, K. Kreis, K. Schwarz, D. Li, R. Rombach, A. Torralba, and S. Fidler, "Neuralfield-ldm: Scene generation with hierarchical latent diffusion models," in *Proceedings of the IEEE/CVF conference on computer vision and pattern recognition*, 2023, pp. 8496–8506.
- [113] J. Wynn and D. Turmukhambetov, "Diffusionerf: Regularizing neural radiance fields with denoising diffusion models," in *Proceedings of the IEEE/CVF Conference on Computer Vision and Pattern Recognition*, 2023, pp. 4180–4189.
- [114] J. Chung, S. Lee, H. Nam, J. Lee, and K. M. Lee, "Luciddreamer: Domain-free generation of 3d gaussian splatting scenes," *arXiv preprint arXiv:2311.13384*, 2023.
- [115] R. Fridman, A. Abecasis, Y. Kasten, and T. Dekel, "Scenescape: Text-driven consistent scene generation," *Advances in Neural Information Processing Systems*, vol. 36, 2024.
- [116] Z. Wu, Y. Li, H. Yan, T. Shang, W. Sun, S. Wang, R. Cui, W. Liu, H. Sato, H. Li *et al.*, "Blockfusion: Expandable 3d scene generation using latent tri-plane extrapolation," *ACM Transactions on Graphics (TOG)*, vol. 43, no. 4, pp. 1–17, 2024.
- [117] G. Gao, W. Liu, A. Chen, A. Geiger, and B. Schölkopf, "Graphdreamer: Compositional 3d scene synthesis from scene graphs," in *Proceedings of the IEEE/CVF Conference on Computer Vision and Pattern Recognition*, 2024, pp. 21 295–21 304.
- [118] J. Tang, Y. Nie, L. Markhasin, A. Dai, J. Thies, and M. Nießner, "Diffuscene: Denoising diffusion models for generative indoor scene synthesis," in *Proceedings of the IEEE/CVF conference on computer vision and pattern recognition*, 2024, pp. 20 507–20 518.
- [119] R. Po and G. Wetzstein, "Compositional 3d scene generation using locally conditioned diffusion," in *2024 International Conference on 3D Vision (3DV)*. IEEE, 2024, pp. 651–663.
- [120] J. Zhang, X. Li, Z. Wan, C. Wang, and J. Liao, "Text2nerf: Text-driven 3d scene generation with neural radiance fields," *IEEE Transactions on Visualization and Computer Graphics*, 2024.
- [121] G. Kim and S. Y. Chun, "Datid-3d: Diversity-preserved domain adaptation using text-to-image diffusion for 3d generative model," in *Proceedings of the IEEE/CVF conference on computer vision and pattern recognition*, 2023, pp. 14 203–14 213.
- [122] A. Mikaeili, O. Perel, M. Safaei, D. Cohen-Or, and A. Mahdavi-Amiri, "Sked: Sketch-guided text-based 3d editing," in *Proceedings of the IEEE/CVF International Conference on Computer Vision*, 2023, pp. 14 607–14 619.
- [123] E. Sella, G. Fiebelman, P. Hedman, and H. Averbuch-Elor, "Vox-e: Text-guided voxel editing of 3d objects," in *Proceedings of the IEEE/CVF International Conference on Computer Vision*, 2023, pp. 430–440.
- [124] X. Han, Y. Cao, K. Han, X. Zhu, J. Deng, Y.-Z. Song, T. Xiang, and K.-Y. K. Wong, "Headsculpt: Crafting 3d head avatars with text," *Advances in Neural Information Processing Systems*, vol. 36, 2024.
- [125] J. Zhuang, C. Wang, L. Lin, L. Liu, and G. Li, "Dreameditor: Text-driven 3d scene editing with neural fields," in *SIGGRAPH Asia 2023 Conference Papers*, 2023, pp. 1–10.
- [126] F.-L. Liu, H. Fu, Y.-K. Lai, and L. Gao, "Sketchdream: Sketch-based text-to-3d generation and editing," *ACM Transactions on Graphics (TOG)*, vol. 43, no. 4, pp. 1–13, 2024.
- [127] Y. Chen, Z. Chen, C. Zhang, F. Wang, X. Yang, Y. Wang, Z. Cai, L. Yang, H. Liu, and G. Lin, "Gaussianeditor: Swift and controllable 3d editing with gaussian splatting," in *Proceedings of the IEEE/CVF Conference on Computer Vision and Pattern Recognition*, 2024, pp. 21 476–21 485.
- [128] K. Pandey, P. Guerrero, M. Gadelha, Y. Hold-Geoffroy, K. Singh, and N. J. Mitra, "Diffusion handles enabling 3d edits for diffusion models by lifting activations to 3d," in *Proceedings of the IEEE/CVF Conference on Computer Vision and Pattern Recognition*, 2024, pp. 7695–7704.
- [129] S. Yoo, K. Kim, V. G. Kim, and M. Sung, "As-plausible-as-possible: Plausibility-aware mesh deformation using 2d diffusion priors," in *Proceedings of the IEEE/CVF Conference on Computer Vision and Pattern Recognition*, 2024, pp. 4315–4324.
- [130] C. Deng, C. Jiang, C. R. Qi, X. Yan, Y. Zhou, L. Guibas, D. Anguelov *et al.*, "Nerdi: Single-view nerf synthesis with language-guided diffusion as general image priors," in *Proceedings of the IEEE/CVF conference on computer vision and pattern recognition*, 2023, pp. 20 637–20 647.
- [131] A. Karnewar, A. Vedaldi, D. Novotny, and N. J. Mitra, "Holodiffusion: Training a 3d diffusion model using 2d images," in *Proceedings of the IEEE/CVF conference on computer vision and pattern recognition*, 2023, pp. 18 423–18 433.
- [132] H.-Y. Tseng, Q. Li, C. Kim, S. Alsisan, J.-B. Huang, and J. Kopf, "Consistent view synthesis with pose-guided diffusion models," in *Proceedings of the IEEE/CVF Conference on Computer Vision and Pattern Recognition*, 2023, pp. 16 773–16 783.
- [133] Z. Zhou and S. Tulsiani, "Sparsefusion: Distilling view-conditioned diffusion for 3d reconstruction," in *Proceedings of the IEEE/CVF Conference on Computer Vision and Pattern Recognition*, 2023, pp. 12 588–12 597.

- [134] R. Liu, R. Wu, B. Van Hoorick, P. Tokmakov, S. Zakharov, and C. Vondrick, “Zero-1-to-3: Zero-shot one image to 3d object,” in *Proceedings of the IEEE/CVF international conference on computer vision*, 2023, pp. 9298–9309.
- [135] E. R. Chan, K. Nagano, M. A. Chan, A. W. Bergman, J. J. Park, A. Levy, M. Aittala, S. De Mello, T. Karras, and G. Wetzstein, “Generative novel view synthesis with 3d-aware diffusion models,” in *Proceedings of the IEEE/CVF International Conference on Computer Vision*, 2023, pp. 4217–4229.
- [136] R. Shi, H. Chen, Z. Zhang, M. Liu, C. Xu, X. Wei, L. Chen, C. Zeng, and H. Su, “Zero123++: a single image to consistent multi-view diffusion base model,” *arXiv preprint arXiv:2310.15110*, 2023.
- [137] D. Watson, W. Chan, R. M. Brualla, J. Ho, A. Tagliasacchi, and M. Norouzi, “Novel view synthesis with diffusion models,” in *The Eleventh International Conference on Learning Representations*, 2023.
- [138] J. Gu, A. Treuithick, K.-E. Lin, J. M. Susskind, C. Theobalt, L. Liu, and R. Ramamoorthi, “Nerfdiff: Single-image view synthesis with nerf-guided distillation from 3d-aware diffusion,” in *International Conference on Machine Learning*. PMLR, 2023, pp. 11 808–11 826.
- [139] L. Höllein, A. Božič, N. Müller, D. Novotny, H.-Y. Tseng, C. Richardt, M. Zollhöfer, and M. Nießner, “Viewdiff: 3d-consistent image generation with text-to-image models,” in *Proceedings of the IEEE/CVF Conference on Computer Vision and Pattern Recognition*, 2024, pp. 5043–5052.
- [140] J. Ye, P. Wang, K. Li, Y. Shi, and H. Wang, “Consistent-1-to-3: Consistent image to 3d view synthesis via geometry-aware diffusion models,” in *2024 International Conference on 3D Vision (3DV)*. IEEE, 2024, pp. 664–674.
- [141] Y. Liu, C. Lin, Z. Zeng, X. Long, L. Liu, T. Komura, and W. Wang, “Syncdreamer: Generating multiview-consistent images from a single-view image,” in *The Twelfth International Conference on Learning Representations*, 2024.
- [142] Y. Ji, Z. Chen, E. Xie, L. Hong, X. Liu, Z. Liu, T. Lu, Z. Li, and P. Luo, “Ddp: Diffusion model for dense visual prediction,” in *Proceedings of the IEEE/CVF International Conference on Computer Vision*, 2023, pp. 21 741–21 752.
- [143] J. Li, Y. Wang, Z. Huang, J. Zheng, K. Xian, Z. Cao, and J. Zhang, “Diffusion-augmented depth prediction with sparse annotations,” in *Proceedings of the 31st ACM International Conference on Multimedia*, 2023, pp. 2865–2876.
- [144] F. Zhang, S. You, Y. Li, and Y. Fu, “Atlantis: Enabling underwater depth estimation with stable diffusion,” in *Proceedings of the IEEE/CVF Conference on Computer Vision and Pattern Recognition*, 2024, pp. 11 852–11 861.
- [145] S. Saxena, C. Herrmann, J. Hur, A. Kar, M. Norouzi, D. Sun, and D. J. Fleet, “The surprising effectiveness of diffusion models for optical flow and monocular depth estimation,” *Advances in Neural Information Processing Systems*, vol. 36, 2024.
- [146] B. Ke, A. Obukhov, S. Huang, N. Metzger, R. C. Daudt, and K. Schindler, “Repurposing diffusion-based image generators for monocular depth estimation,” in *Proceedings of the IEEE/CVF Conference on Computer Vision and Pattern Recognition*, 2024, pp. 9492–9502.
- [147] Z. Wu, S. Song, A. Khosla, F. Yu, L. Zhang, X. Tang, and J. Xiao, “3d shapenets: A deep representation for volumetric shapes,” in *Proceedings of the IEEE conference on computer vision and pattern recognition*, 2015, pp. 1912–1920.
- [148] S. Choi, Q.-Y. Zhou, S. Miller, and V. Koltun, “A large dataset of object scans,” *arXiv preprint arXiv:1602.02481*, 2016.
- [149] L. Pan, T. Wu, Z. Cai, Z. Liu, X. Yu, Y. Rao, J. Lu, J. Zhou, M. Xu, X. Luo *et al.*, “Multi-view partial (mvp) point cloud challenge 2021 on completion and registration: Methods and results,” *arXiv preprint arXiv:2112.12053*, 2021.
- [150] L. P. Tchampi, V. Kosaraju, H. Rezatofighi, I. Reid, and S. Savarese, “Topnet: Structural point cloud decoder,” in *Proceedings of the IEEE/CVF conference on computer vision and pattern recognition*, 2019, pp. 383–392.
- [151] K. Park, K. Rematas, A. Farhadi, and S. M. Seitz, “Photoshape: Photorealistic materials for large-scale shape collections,” *arXiv preprint arXiv:1809.09761*, 2018.
- [152] J. Collins, S. Goel, K. Deng, A. Luthra, L. Xu, E. Gundogdu, X. Zhang, T. F. Y. Vicente, T. Dideriksen, H. Arora *et al.*, “Abo: Dataset and benchmarks for real-world 3d object understanding,” in *Proceedings of the IEEE/CVF conference on computer vision and pattern recognition*, 2022, pp. 21 126–21 136.
- [153] B. Calli, A. Singh, A. Walsman, S. Srinivasa, P. Abbeel, and A. M. Dollar, “The ycb object and model set: Towards common benchmarks for manipulation research,” in *2015 international conference on advanced robotics (ICAR)*. IEEE, 2015, pp. 510–517.
- [154] J. Reizenstein, R. Shapovalov, P. HENZLER, L. Sbordone, P. Labatut, and D. Novotny, “Common objects in 3d: Large-scale learning and evaluation of real-life 3d category reconstruction,” in *Proceedings of the IEEE/CVF international conference on computer vision*, 2021, pp. 10901–10911.
- [155] M. Deitke, D. Schwenk, J. Salvador, L. Weihs, O. Michel, E. Vander-Bilt, L. Schmidt, K. Ehsani, A. Kembhavi, and A. Farhadi, “Objaverse: A universe of annotated 3d objects,” in *Proceedings of the IEEE/CVF Conference on Computer Vision and Pattern Recognition*, 2023, pp. 13 142–13 153.
- [156] L. Downs, A. Francis, N. Koenig, B. Kinman, R. Hickman, K. Reymann, T. B. McHugh, and V. Vanhoucke, “Google scanned objects: A high-quality dataset of 3d scanned household items,” in *2022 International Conference on Robotics and Automation (ICRA)*. IEEE, 2022, pp. 2553–2560.
- [157] T. Luo, C. Rockwell, H. Lee, and J. Johnson, “Scalable 3d captioning with pretrained models,” *Advances in Neural Information Processing Systems*, vol. 36, 2024.
- [158] K. Chen, C. B. Choy, M. Savva, A. X. Chang, T. Funkhouser, and S. Savarese, “Text2shape: Generating shapes from natural language by learning joint embeddings,” in *Computer Vision—ACCV 2018: 14th Asian Conference on Computer Vision, Perth, Australia, December 2–6, 2018, Revised Selected Papers, Part III 14*. Springer, 2019, pp. 100–116.
- [159] H. Fu, R. Jia, L. Gao, M. Gong, B. Zhao, S. Maybank, and D. Tao, “3d-future: 3d furniture shape with texture,” *International Journal of Computer Vision*, vol. 129, pp. 3313–3337, 2021.
- [160] T. Wu, J. Zhang, X. Fu, Y. Wang, J. Ren, L. Pan, W. Wu, L. Yang, J. Wang, C. Qian *et al.*, “Omniobject3d: Large-vocabulary 3d object dataset for realistic perception, reconstruction and generation,” in *Proceedings of the IEEE/CVF Conference on Computer Vision and Pattern Recognition*, 2023, pp. 803–814.
- [161] M. A. Uy, Q.-H. Pham, B.-S. Hua, T. Nguyen, and S.-K. Yeung, “Revisiting point cloud classification: A new benchmark dataset and classification model on real-world data,” in *Proceedings of the IEEE/CVF international conference on computer vision*, 2019, pp. 1588–1597.
- [162] Renderpeople. (2024) World’s largest 3d people library. [Online]. Available: <https://renderpeople.com/>
- [163] T. Yu, Z. Zheng, K. Guo, P. Liu, Q. Dai, and Y. Liu, “Function4d: Real-time human volumetric capture from very sparse consumer rgbd sensors,” in *IEEE Conference on Computer Vision and Pattern Recognition (CVPR2021)*, June 2021.
- [164] R. Bashirov, A. Ianina, K. Isakov, Y. Kononenko, V. Strizhkova, V. Lempitsky, and A. Vakhitov, “Real-time rgbd-based extended body pose estimation,” in *Proceedings of the IEEE/CVF winter conference on applications of computer vision*, 2021, pp. 2807–2816.
- [165] C. Guo, S. Zou, X. Zuo, S. Wang, W. Ji, X. Li, and L. Cheng, “Generating diverse and natural 3d human motions from text,” in *Proceedings of the IEEE/CVF Conference on Computer Vision and Pattern Recognition*, 2022, pp. 5152–5161.
- [166] N. Mahmood, N. Ghorbani, N. F. Troje, G. Pons-Moll, and M. J. Black, “Amass: Archive of motion capture as surface shapes,” in *Proceedings of the IEEE/CVF international conference on computer vision*, 2019, pp. 5442–5451.
- [167] C. Guo, X. Zuo, S. Wang, S. Zou, Q. Sun, A. Deng, M. Gong, and L. Cheng, “Action2motion: Conditioned generation of 3d human motions,” in *Proceedings of the 28th ACM International Conference on Multimedia*, 2020, pp. 2021–2029.
- [168] Y. Ji, F. Xu, Y. Yang, F. Shen, H. T. Shen, and W.-S. Zheng, “A large-scale varying-view rgb-d action dataset for arbitrary-view human action recognition,” *arXiv preprint arXiv:1904.10681*, 2019.
- [169] H. Yang, H. Zhu, Y. Wang, M. Huang, Q. Shen, R. Yang, and X. Cao, “Facescape: A large-scale high quality 3d face dataset and detailed riggable 3d face prediction,” in *IEEE/CVF Conference on Computer Vision and Pattern Recognition (CVPR)*, June 2020.
- [170] H.-I. Ho, L. Xue, J. Song, and O. Hilliges, “Learning locally editable virtual humans,” in *Proceedings of the IEEE/CVF Conference on Computer Vision and Pattern Recognition*, 2023, pp. 21 024–21 035.
- [171] Q. Ma, J. Yang, A. Ranjan, S. Pujades, G. Pons-Moll, S. Tang, and M. J. Black, “Learning to dress 3d people in generative clothing,” in *Proceedings of the IEEE/CVF Conference on Computer Vision and Pattern Recognition*, 2020, pp. 6469–6478.
- [172] M. Kaufmann, J. Song, C. Guo, K. Shen, T. Jiang, C. Tang, J. J. Zárate, and O. Hilliges, “Emdb: The electromagnetic database of global 3d human pose and shape in the wild,” in *Proceedings of the*

- IEEE/CVF International Conference on Computer Vision*, 2023, pp. 14 632–14 643.
- [173] J. Straub, T. Whelan, L. Ma, Y. Chen, E. Wijmans, S. Green, J. J. Engel, R. Mur-Artal, C. Ren, S. Verma *et al.*, “The replica dataset: A digital replica of indoor spaces,” *arXiv preprint arXiv:1906.05797*, 2019.
- [174] H. Fu, B. Cai, L. Gao, L.-X. Zhang, J. Wang, C. Li, Q. Zeng, C. Sun, R. Jia, B. Zhao *et al.*, “3d-front: 3d furnished rooms with layouts and semantics,” in *Proceedings of the IEEE/CVF International Conference on Computer Vision*, 2021, pp. 10 933–10 942.
- [175] A. Geiger, P. Lenz, and R. Urtasun, “Are we ready for autonomous driving? the kitti vision benchmark suite,” in *2012 IEEE conference on computer vision and pattern recognition*. IEEE, 2012, pp. 3354–3361.
- [176] I. Armeni, O. Sener, A. R. Zamir, H. Jiang, I. Brilakis, M. Fischer, and S. Savarese, “3d semantic parsing of large-scale indoor spaces,” in *Proceedings of the IEEE conference on computer vision and pattern recognition*, 2016, pp. 1534–1543.
- [177] P. Ammirato, P. Poirson, E. Park, J. Košecká, and A. C. Berg, “A dataset for developing and benchmarking active vision,” in *2017 IEEE International Conference on Robotics and Automation (ICRA)*. IEEE, 2017, pp. 1378–1385.
- [178] J. McCormac, A. Handa, S. Leutenegger, and A. J. Davison, “Scenenet rgb-d: 5m photorealistic images of synthetic indoor trajectories with ground truth,” *arXiv preprint arXiv:1612.05079*, 2016.
- [179] S. Song, S. P. Lichtenberg, and J. Xiao, “Sun rgb-d: A rgb-d scene understanding benchmark suite,” in *Proceedings of the IEEE conference on computer vision and pattern recognition*, 2015, pp. 567–576.
- [180] H. Caesar, V. Bankiti, A. H. Lang, S. Vora, V. E. Liong, Q. Xu, A. Krishnan, Y. Pan, G. Baldan, and O. Beijbom, “nusenes: A multimodal dataset for autonomous driving,” in *Proceedings of the IEEE/CVF conference on computer vision and pattern recognition*, 2020, pp. 11 621–11 631.
- [181] P. Sun, H. Kretzschmar, X. Dotiwalla, A. Chouard, V. Patnaik, P. Tsui, J. Guo, Y. Zhou, Y. Chai, B. Caine *et al.*, “Scalability in perception for autonomous driving: Waymo open dataset,” in *Proceedings of the IEEE/CVF conference on computer vision and pattern recognition*, 2020, pp. 2446–2454.
- [182] Y. Yao, Z. Luo, S. Li, J. Zhang, Y. Ren, L. Zhou, T. Fang, and L. Quan, “Blendedmvs: A large-scale dataset for generalized multi-view stereo networks,” in *Computer Vision and Pattern Recognition (CVPR)*, 2020.
- [183] T. Zhou, R. Tucker, J. Flynn, G. Fyffe, and N. Snavely, “Stereo magnification: Learning view synthesis using multiplane images,” *arXiv preprint arXiv:1805.09817*, 2018.
- [184] A. Chang, A. Dai, T. Funkhouser, M. Halber, M. Niessner, M. Savva, S. Song, A. Zeng, and Y. Zhang, “Matterport3d: Learning from rgb-d data in indoor environments,” *International Conference on 3D Vision (3DV)*, 2017.
- [185] V. Guizilini, R. Ambrus, S. Pillai, A. Raventos, and A. Gaidon, “3d packing for self-supervised monocular depth estimation,” in *Proceedings of the IEEE/CVF conference on computer vision and pattern recognition*, 2020, pp. 2485–2494.
- [186] M. Roberts, J. Ramapuram, A. Ranjan, A. Kumar, M. A. Bautista, N. Paczan, R. Webb, and J. M. Susskind, “Hypersim: A photorealistic synthetic dataset for holistic indoor scene understanding,” in *Proceedings of the IEEE/CVF international conference on computer vision*, 2021, pp. 10 912–10 922.